YSSP25

A new generation of scientists

Proceedings of the Final Colloquium

Young Scientists Summer Program

International Institute for Applied Systems Analysis
IIASA www.iiasa.ac.at

IIASA's annual three-month Young Scientists Summer Program (YSSP) offers research opportunities to talented young researchers whose interests correspond with IIASA's ongoing research on issues of global environmental, economic, and social change. From June through August each year participants work within the Institute's research programs under the guidance of IIASA scientific staff.

The Proceedings of the Final Presentations comprises summaries of the research results obtained during the YSSP that were presented at International Institute for Applied Systems Analysis, Laxenburg, Austria, on 21–22 August 2025.

The Proceedings are the sole work of the authors with limited review by their IIASA mentors or any other staff of the Institute. They are not for publication in the current form. Views or opinions expressed herein do not necessarily represent those of the Institute, its National Member Organizations, or other organizations supporting the work. This compilation contains all the summaries available at the time of finalization of the Proceedings.

Proceedings Editors: Rasheed Akinleye Hammed (BNR), **Samantha Kloft** (ASA)**, Steffen Lohrey** (ECE)**, Shreeyash Malode** (ECE)**, Daniel Itzamna Avila Ortega** (ASA)**, Daria Turavinina** (POPJUS)**, Terrance Wang** (BNR)**, and Brian D. Fath**

DAY 1	
	WODAK Room
Session 1	**Chair: Michael Freiberger**
10:30 – 12:00	**1) Daria Turavanina -** Educational inequalities and vaccine hesitancy under covid-19 restrictions in Western Europe **2) Veronika Schick -** Burdens for some, benefits for others - Distributive preferences in natural hazard management **3) Hang Thanh Ngo -** Characterizing and assessing compound climate risks in the United States **4) Abbie Robinson -** Immigration and changing disparities in heat exposure in the US since 1980 **5) Tam Nguyen -** Modelling flood-induced displacement and vulnerability in Africa **6) Ebere Nnanwube -** Policy actions for instituting gender equality & equity in landfill waste picking of Lagos State, Nigeria. **7) Hadi Prasojo -** Green securities as financial tools for the transition: A macro perspective **8) Guo-Liang Zheng - '**Double-edged' solar geoengineering: Impacts and responses for termination shock risks
	LUNCH
Session 2	**Chair: Adriana Gomez Sanabria**
13:45 – 15:15	**1) Camille Wejnert-Depue -** Exploring the links between carbon management technologies (CMTs) and multidimensional wellbeing in mitigation pathways **2) Jack Vahnberg -** Producing poverty: studying the winners and losers of energy provision through the case of Swedish district heating **3) Shreeyash Malode -** Sectoral emissions trading in national energy systems model: application to Indian cement and steel sector using MESSAGEix framework **4) Edita Dvořáková** - Linking social and environmental impacts within the urban system **5) Shu Nawawi** - Modeling building stock transitions in a changing climate and energy systems: Balancing decarbonization and well-being **6) Poornima Kumar -** Exploring the indirect energy impacts of digitalised daily life: A test case of smart heating using the FeliX model **7) Yuezhang He -** Leveraging temporal and spatial flexibility of renewable-centric data centers in China **8) Koga Yamazaki -** The impact of changes in nitrogen gas emission in climate change mitigation scenarios on air quality in eastern Asia
	BREAK
Session 3	**Chair: Caroline Zimm**
15:45 – 17:15	**1) Jianxiang Shen -** Plant-level decarbonization strategies for power, iron & steel, and cement sectors in China considering health co-benefits **2) Ji Soo Kim -** The effectiveness of the ASEAN Agreement on transboundary haze pollution **3) Steffen Lohrey -** Temperature extremes and societal response **4) Yixu He -** Assessing the impact of compound drought-heatwave events on hydroelectric and thermal power generation **5) Parisa Javadi -** The role of land and ocean-based geochemical CO_2 removal pathways in climate mitigation **6) Shuting Fan -** Unlocking low-carbon potential: how international climate finance shapes the cost of capital and global decarbonization pathways

	7) Jana Fakhreddine - Multi-model analysis of global hydrogen trade development in a low-carbon energy system **8) Sara Nazari -** Developing a global groundwater risk assessment framework

DAY 2	
	WODAK Room
08:45 – 09:00	**Opening remarks: Fabian Wagner and Brian Fath**
Session 4	**Chair: Dor Fridman**
09:00 – 10:30	**1) Gabriel Stecher -** Evaluating the climate resilience of agricultural management practices for improving water quality in Uganda **2) Weiyi Gu -** Mapping cost-effective adaptation pathways to global quantity- and quality-induced agricultural water scarcity **3) Adham Badawy -** Opening pathways: How infrastructure investment reduces inequality in agricultural adaptation choices **4) Avijit Pandit -** Beyond the representative consumer: European dietary change scenarios with demographic disaggregation **5) Sanda Ny Avo -** Disaggregating non-renewable energy use in EU agriculture: an activity-level allocation based on recent econometric modelling **6) Flavia Aschi -** Bending the curve 2.0 – Updates on the modelling protocol. Note for IAM and BDM modellers **7) Terrance Wang -** Diagnosing declines in marine biodiversity **8) Junjie Liu -** Are global protected areas effective? Evidence from counterfactual matching of camera trap data **9) Tom Hackbarth -** Designing nature-positive pathways for Europe's people and biodiversity
	BREAK
Session 5	**Chair: Piotr Zebrowski**
11:00 – 12:30	**1) Ville Tuominen -** Peatland drought resilience in future climate in Europe **2) Rasheed Akinleye Hammed -** Modelling the influence of grazing on regional wildfire dynamics in Europe **3) Bin Du -** From fields to future: A machine learning framework for sustainable carbon and nitrogen management in pan-European agriculture **4) Jim Allansson -** The role of forestry biomass in the emerging fossil free iron and steel making process **5) Ross Tieman -** Algorithmic complexity-based methods for assessing social-ecological system resilience **6) Samantha Kloft -** Intersectional influences on trust in public health authorities: insights from a U.S. nationally representative sample **7) Joaquín Rodrigo de la Barra Toloza -** Enhancing critical infrastructure networks resilience against extreme weather events using multicriteria portfolio decision analysis **8) Xinyu Zhang -** A novel single and double-cropping rice mapping method by integrating phenology knowledge and deep learning without current-year ground samples
	LUNCH

Session 6	Chair: Brian Fath
14:00 – 15:30	1) **Florian Weidinger-** How intensively are Europe's forests used? Towards a database and framework for tracking indicators, addressing uncertainty, and capturing change 2) **Ana Paula Matos e Silva -** Analyzing requirements for an accurate land cover data collection by visual interpretation of various sources of images 3) **Zhenjun Zhang -** Revealing the indirect impacts of climate change on high-latitude countries: An integrated climate and economic model approach 4) **Yuqin Lai -** Forest age dynamics in OSCAR: Improving land use emission estimates and reconciliation with national inventories 5) **Protus Kyalo -** Modelling semi-arid ecosystem processes in Baringo County, Kenya using the BGC MAN Model 6) **Daniel Itzamna Avila Ortega -** Sustainable agriculture and planetary boundaries: Exploring the socioeconomic and socio-ecological footprints of Mexico's agricultural sector 7) **Anzhelika Slobodian -** Demand-side flexibility for balancing microgrids in islanded mode: Engaging local consumers in resilient energy transitions 8) **John Lind -** Social-ecological network analysis of meadow governance in Sweden **CLOSE OF PROGRAM – RECEPTION IN CONFERENCE AREA**

Contents

Population and Just Societies

(POPJUS)

Educational inequalities and vaccine hesitancy under Covid-19 restrictions in Western Europe

Daria Turavinina, Chulalongkorn University, Thailand
Email: darіaturavininaal@gmail.com
IIASA Mentors: Sergei Scherbov (POPJUS) and Daniela Weber (POPJUS)

Introduction. This study investigates the relationship between the severity of experienced COVID-19 restrictions and vaccine hesitancy in Western Europe and examines how education moderates this association. Stringent restrictions were hypothesised to trigger psychological reactance (Brehm & Brehm, 2013) and reduce confidence in vaccines, a phenomenon moderated by the level of education.

Methodology. Individual-level data from the ISSP *Health and Healthcare II* (2021–22; ~10,000 respondents across nine Western European democracies) were merged with country-level COVID-19 restriction indicators from the Oxford Government Response Tracker. Vaccine hesitancy was coded in three categories (agree, neutral, disagree). The main predictor was the 2020 mean stringency index (grouped into low, medium, high). Education was grouped into low, medium, and high. Multinomial logistic regressions with random intercepts for countries were estimated, controlling for demographic and socioeconomic factors. Additional models tested specific policy domains and conducted robustness cheks, including recent changes in strinegncy and the effect of comptemporaneous mortality.

Results. Higher stringency in 2020 was initially associated with stronger vaccine hesitancy across all education groups, particularly among those with lower education. Workplace closures, stay-at-home orders, and limits on public gatherings showed the clearest associations. However, once national COVID-19 mortality rates were included, the relationship between recent stringency dynamics and vaccine hesitancy was no longer statistically significant, suggesting that observed effects may be shaped more by contextual severity rather than psychological reactance.

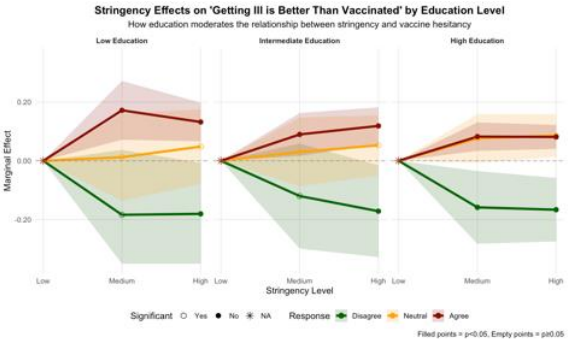

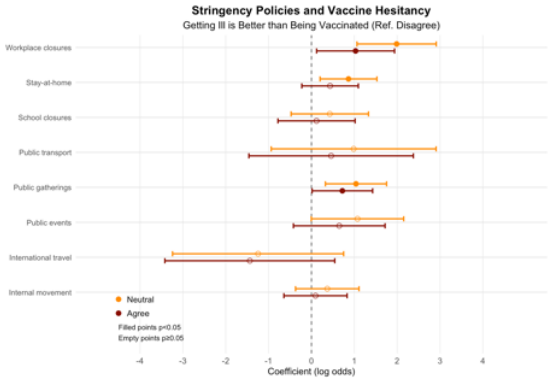

Conclusions. While stricter restrictions appeared to coincide with greater vaccine hesitancy, especially among less-educated respondents, these associations weakened after accounting for pandemic mortality.

References.

1. Brehm, S. S., & Brehm, J. W. (2013). *Psychological reactance: A theory of freedom and control*. Academic Press.

Benefits for some, burdens for others – distributive preferences in natural hazard management

Veronika Schick, ETH Zurich, Switzerland
Email: vschick@ethz.ch
IIASA Mentors: Elliott Woodhouse (POPJUS), Thomas Schinko (POPJUS)

Introduction. Switzerland is warming at twice the global rate, intensifying natural hazards like floods, debris flows and landslides[1]. The 2025 Blatten landslide exemplifies the urgent need for climate adaptation and raises critical questions of who pays, and which regions specifically should benefit from protection. This study explores publicly acceptable policy options for distributing costs and benefits of adaptation. Given Switzerland's high level of political polarization[2], we analyze preferences among socio-culturally conservative and progressive groups within Switzerland to identify which policy options are broadly supported and which are polarized.

Methodology. We conducted a conjoint survey experiment with a representative sample of 900 Swiss residents in May 2025. The experiment included three attributes: (1) who should pay for adaptation, (2) who should be exempted from costs, and (3) which municipalities should receive targeted protection. To assess socio-cultural attitudes, we measured respondents' values and their perceived affiliations with specific societal groups, combining these into a composite index. To compare preferences across socio-culturally progressive and conservative groups, we calculated Marginal Means for each group, which reflect the average level of support for each policy option.

Results. When it comes to distributing costs, both socio-culturally progressive and conservative groups support redistributive schemes, such as exemptions for low-income individuals. However, progressives show stronger support for redistribution overall. A key point of divergence is the "polluter pays" principle. Progressives support the idea that companies responsible for CO_2 emissions should help cover the costs of natural hazard protection, but they don't think individuals should pay based on their emissions. Conservatives tend to reject both ideas and instead favor requiring those who directly benefit from protective measures, such as residents in hazard-prone areas, to contribute financially. Regarding benefit distribution, there is broad agreement on prioritizing municipalities most affected by natural hazards and ensuring equal protection across regions. However, conservatives are more supportive of giving special protection to municipalities where people have lived for many years, while progressives tend to oppose this idea.

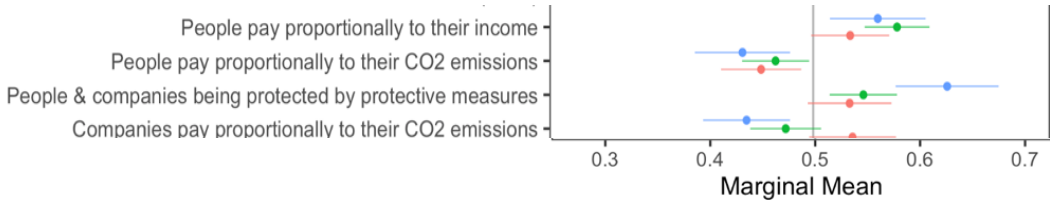

Fig 1. Average support for cost distribution schemes by socio-cultural group (red = progressive, blue = conservative, green =

Conclusions. These insights suggest that viable policy compromises are possible—particularly those that combine perceived financial justice with targeted protection. Integrating these preferences into policy design can help build societal consensus and enhance the legitimacy of climate adaptation efforts.

References

1. IEA. (2022). *Switzerland Climate Resilience Policy Indicator*.
2. Bornschier, S., Häusermann, S., Zollinger, D., & Colombo, C. (2021). How "Us" and "Them" Relates to Voting Behavior—Social Structure, Social Identities, and Electoral Choice. *Comparative Political Studies*, *54*(12), 2087–2122.

Characterizing and assessing compound climate risks in the United States

Hang Ngo, New York University, USA
Email: htn237@nyu.edu
IIASA Mentors: Josephine Borghi (POPJUS) and Robert Šakić Trogrlić (ASA)

Introduction. Compound climate events are becoming increasingly frequent due to climate change. These events arise from interactions among multiple climate hazards and/or drivers such as extreme heat and precipitation that co-occur or compound over space and time. Such events can disrupt health systems and cause significant loss of life and harms to health that exceed individual hazards. Despite this, most current risk assessments focus on single hazards. To address this gap, this study develops an agent-based model (ABM) for the U.S, to explore how risk driver dynamics shape compound climate risks to health and health systems, and to identify populations most affected.

Methodology. We operationalized the IPCC risk framework, as extended by Simpson et al., 2021 for complex climate change risk assessment, to develop a U.S. focused ABM. The model simulates how dynamics among compound climate hazards (extreme heat and precipitation), exposure, sociodemographic and health-related vulnerability, and hospital system response generate emergent compound climate risks to health and health systems, specifically mortality and hospital utilization. Agents represent heterogeneous individuals and hospitals. We developed a stylized prototype in NetLogo to test core dynamics, which will be scaled to the national county level using nationwide data from 2005-2022 including historical climate data, sociodemographic information, environmental justice indicators, and health outcome data. The study will also map and quantify compound climate risk scores to identify hotspots and populations most affected at subnational levels.

Results. The ABM simulation captures three core dynamic processes: (1) differential and evolving vulnerability, (2) agent exposure to compound climate hazards, and (3) stress on hospital systems. The model comprises modules for compound climate hazard interactions, population and hospital exposure, adverse health impacts and hospital utilization, and hospital system capacity and response. Outputs generated from the model provide insights into how interactions between agent vulnerability and hazard exposure drive differential mortality risk and hospital utilization. The model will also capture how vulnerability evolves with continued exposure, while feedback loops illustrate how hospital system capacity mediates mortality risk under increasing system stress.

Conclusions. This study is critical for characterizing and assessing complex, compound climate risks to health and health systems. The ABM provides actionable insights to guide integrative-risk management strategies for promoting health and health systems resilience, particularly for informing how, where, and for whom adaptation and disaster risk reduction efforts are most urgently needed to protect population health and communities on the frontlines of climate change.

References

Simpson, N. P., Mach, K. J., Constable, A., Hess, J., Hogarth, R., Howden, M., Lawrence, J., Lempert, R. J., Muccione, V., Mackey, B., New, M. G., O'Neill, B., Otto, F., Pörtner, H.-O., Reisinger, A., Roberts, D., Schmidt, D. N., Seneviratne, S., Strongin, S., Trisos, C. H. (2021). A framework for complex climate change risk assessment. *One Earth*, *4*(4), 489–501. https://doi.org/10.1016/j.oneear.2021.03.005
Zscheischler, J., Martius, O., Westra, S., Bevacqua, E., Raymond, C., Horton, R. M., van den Hurk, B., AghaKouchak, A., Jézéquel, A., Mahecha, M. D., Maraun, D., Ramos, A. M., Ridder, N. N., Thiery, W., & Vignotto, E. (2020). A typology of compound weather and climate events. *Nature Reviews. Earth & Environment*, *1*(7), 333–347. https://doi.org/10.1038/s43017-020-0060-z

Immigration and changing heat exposure disparities in the United States since 1980

Abbie Robinson, The Pennsylvania State University, United States
Email: afr5774@psu.edu
IIASA Mentors: Lisa Thalheimer (POPJUS) and Gregor Zens (POPJUS)

Introduction. The extent of heat exposure across a population is shaped by the interplay between climatic and demographic change, yet the relative contribution of each remains unclear. Prior research on this topic has used decomposition as a demographic method to break down the change in aggregated heat-related outcomes by isolating temperature and population effects (Carr et al., 2024; Park et al., 2020). No study, however, has examined nativity-based differences in exposure to excess heat in the United States. We use decomposition methods to address two research objectives. First, we estimate how shifts in local temperature and the geographic distribution of the (non)immigrant population contribute to changes in heat exposure in the continental United States from 1980 to 2020. Second, we evaluate heterogeneity in these changes by spatial and demographic variables (i.e., US census division, metropolitan status, region of origin).

Methodology. Our decomposition analysis follows five steps. First, we access five decades of National Historical Geographic Information System (NHGIS) census data. These records include geographic identifiers that enable linkage to temperature estimates produced by the Parameter-elevation Regressions on Independent Slopes Model (PRISM). Second, we calculate observed heat exposure by multiplying the local temperature by the proportion of the focal population of the given decennial year. Third, we sum these products across counties to obtain a population-weighted average temperature. Fourth, we generate counterfactual heat exposures using the same weighted averaging procedure. Finally, we decompose the total change in observed exposure into additive components: (1) a temperature effect, which estimates the average change in exposure that would occur if population distributions remained fixed, and (2) a population redistribution effect, which estimates the average change in exposure holding temperature constant.

Results. Immigrants have consistently experienced higher summer (June-August) heat exposure than US-born individuals since 1990. According to our decomposition, the overall increase in exposure (for both populations) is driven more by changes in where people live than by summer temperatures. For example, the 1.03 °C increase in foreign-born exposure is largely attributable to a population redistribution effect (0.94), with a smaller effect of rising temperature (0.09). Exploring spatial heterogeneity, however, reveals notable variation across census divisions. Among those with the largest changes, a dominant cooling effect decreased exposure in the East South Central region, while immigrant redistribution increased exposure in the Mountain region. Shifts in population distribution additionally shape foreign-born exposure by region of origin and metropolitan residence.

Conclusions. The decomposition results point to three main takeaways. First, place of residence is the primary contributor to overall higher heat exposure among the foreign-born population. With clear inequalities by nativity, settlement patterns, and not temperature change alone, play a critical role in shaping immigrant heat vulnerability. Second, regional differences in exposure reveal that heat vulnerability in the US is not uniformly worsening. Our census division-specific models unmask important spatial heterogeneity, as we find increased heat exposure in traditionally cooler regions, alongside a dominant cooling trend in southern divisions. Third, the underlying mechanisms of population change require deeper investigation. Future research should explore determinants of residential (im)mobility to inform mitigation strategies that reflect population change and spatial patterns of warming, ensuring equitable policy responses to US heat exposure.

References

Carr, D., Falchetta, G., & Sue Wing, I. (2024a). Population aging and heat exposure in the 21st century: which US regions are at greatest risk and why?. The Gerontologist, 64(3), gnad050.

Park, C. E., Jeong, S., Harrington, L. J., Lee, M. I., & Zheng, C. (2020). Population ageing determines changes in heat vulnerability to future warming. Environmental Research Letters, 15(11), 114043.

Modelling flood-induced displacement and vulnerability in Africa

Ho-Minh-Tam Nguyen, Korea Advanced Institute of Science and Technology, Republic of Korea
Email: hmtnguyen@kaist.ac.kr
IIASA Mentors: Roman Hoffmann (POPJUS) and Timothy Foreman (POPJUS)

Introduction. Floods have become a major driver of displacement, leading to the loss of housing, livelihoods, and infrastructure, and creating prolonged humanitarian challenges (IPCC 2022). Africa, which is composed largely of low- and middle-income countries, bears a disproportionate share of these impacts. By combining a satellite-based, high-resolution (30 m) flood dataset with subnational displacement data from the Internal Displacement Monitoring Centre, this study examines patterns of flood-induced displacement in Africa and evaluates how social vulnerability factors shape these impacts.

Methodology. To align the flood data with displacement records, we performed a spatial integration using a 50 km buffer around each flood pixel to capture associated displacement points. We then applied a Hurdle model to quantify the influence of flooding on displacement across all first-level administrative units in Africa. In the first stage, a logistic regression estimated the probability of any displacement event, with the binary outcome regressed on log-transformed flood exposure. In the second stage, conditional on positive displacement, a linear model was fitted to the log-transformed displacement counts using the same predictors. The unconditional expected displacement was calculated as the product of the predicted probability from the first stage and the expected magnitude from the second stage, allowing separate interpretation of flood effects on both the occurrence and the severity of displacement.

Results. The results reveal substantial heterogeneity in the relationship between flood exposure and displacement magnitude across Africa (Fig. 1). Greater flood exposure is associated with larger displacement events ($\beta > 0$) in the Sahel–Sudan belt, the Horn and East Africa corridor and southern basins. These regions are characterized by extensive floodplains and riverine systems, which contribute to higher displacement severity. In contrast, parts of the Gulf of Guinea and several West African coastal units exhibit mixed or negative effects, indicating that floods in these areas do not always result in higher displacement.

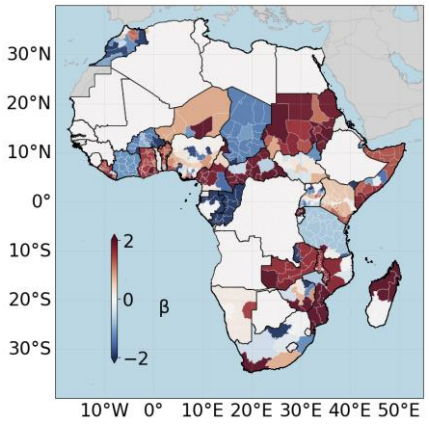

Figure 1. Flood effect on displacement magnitude

Conclusions. This study presents the first framework that integrates high spatio-temporal resolution flood data with displacement records to identify African hotspots of flood-induced displacement. The Sahel–Sudan belt, parts of East Africa, and several southern river basins show particularly severe impacts, underscoring the need for targeted policies, adaptive infrastructure, and community-based risk reduction to mitigate displacement risk.

References

IPCC (2022). Climate Change 2022: Impacts, Adaptation, and Vulnerability. Contribution of Working Group II to the Sixth Assessment Report of the Intergovernmental Panel on Climate Change (Pörtner H-O, Roberts DC, Tignor M, Poloczanska ES, Mintenbeck K, Alegría A, Craig M, Langsdorf S, Löschke S, Möller V, Okem A & Rama B, eds). Cambridge University Press, Cambridge, UK.

Policy actions for instituting gender equality & equity in landfill waste picking of Lagos State, Nigeria

Ebere Florence Nnanwube, University of Ibadan, Oyo State, Nigeria
Email: ennanwube2932@stu.ui.edu.ng
IIASA Mentors: Caroline Zimm (POPJUS), Susanne Hanger-Kopp (POPJUS), Adriana Gomez (ECE)

Introduction. Given the global call for pollution control and low availability of decent jobs, many unskilled people found alternative livelihoods in waste picking. In Lagos State, landfill waste picking is shrouded in gender-based discrimination, where men gate-keep access to valuable waste and women are totally or partially excluded. This study developed an egalitarian model to curb gender discrimination in Lagos landfill waste picking.

Methodology. The study adopted a multi-methods exploratory approach involving four-level stakeholder engagement, including landfill waste pickers via 40 interviews; international experts via 3 expert interviews, local intermediary actors via 3 key informant interviews, and desk reviews. An inductive thematic analysis was conducted and aided by NVivo software.

Results. A Kumu map was designed to serve as an ideal model showing stakeholder relationships and actions for mainstreaming gender in landfill waste picking below:

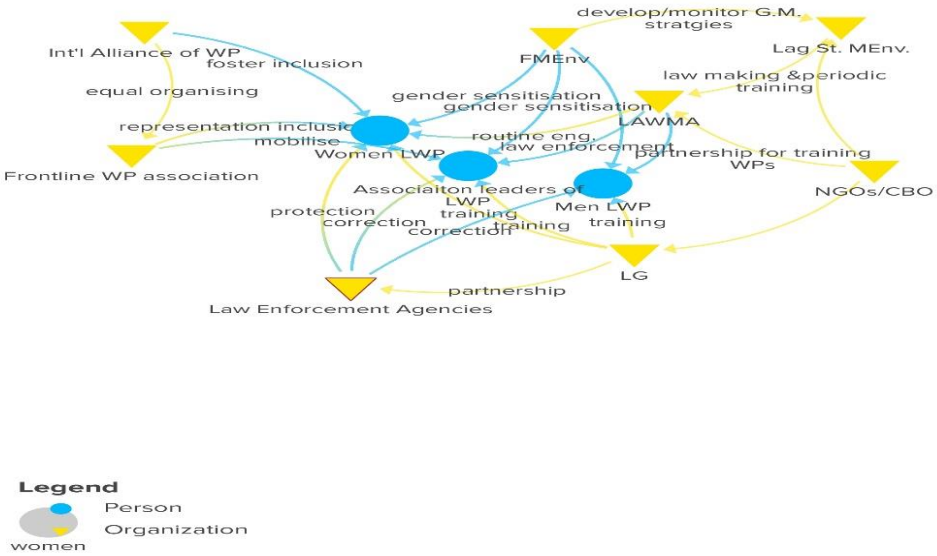

Figure 1. Ideal stakeholder interaction model for landfill gender mainstreaming in Lagos State.

This aided specific policy recommendations. For instance, the federal and Lagos state apex environmental agencies can revisit pages 81-82 of the National Policy on Solid Waste Management (2020) to develop and domesticate gender mainstreaming strategies in the solid waste sector.

Conclusions. This study created practical solutions to gender-based discrimination in Lagos State landfill waste picking by mapping the roles of government and non-government actors towards achieving this.

Economic Frontiers
(EF)

Green securities as financial tools for the transition: a macro perspective

Hadi Prasojo, IUSS Pavia & University of Insubria, Italy
Email: hadi.prasojo@iusspavia.it
IIASA Mentor: Ibrahim Tahri (EF) and Luca Fierro (ASA)

Introduction. Despite high investor interest in green assets, current investment flows remain inadequate to achieve global climate goals. Financial innovations such as securitization may help bridge this gap by aggregating and de-risking green projects, thereby improving their attractiveness to institutional investors. By converting assets into tradable asset-backed securities (ABSs), securitization expands funding access for sustainable projects and spreads credit risk. While green securitizations offer clear benefits, the securitizations role in the 2008 financial crisis highlights the need for caution. They should be viewed as complementary tools within a broader policy and financial framework. This study simulates macro-financial dynamics to assess their role in an orderly transition.

Methodology. To assess the impact of green securitizations on macro-financial dynamics, this study employs Agent-Based Stock-Flow Consistent (AB-SFC) models (Botta et al., 2021, 2024), a comprehensive macroeconomic framework that already incorporates securitization mechanisms. The model is further extended to capture non-financial firms' investment and capital activities, divided into green and conventional (brown) categories. Following Dafermos et al. (2017), firms' green investment shares in total desired investment are derived from their preferences (β_0) and the relative cost of external funding (β_1), with interest-rate sensitivity varying across contexts.

Results. As expected with securitization process, loan volumes increased relative to the no-securitization baseline because banks freed up balance-sheet capacity. This expansion translated into higher green investment. The issuance of asset-backed securities (ABS) also reduced unemployment compared with the alternative scenario, but it raised inequality, as shown by a higher Gini index for household net income.

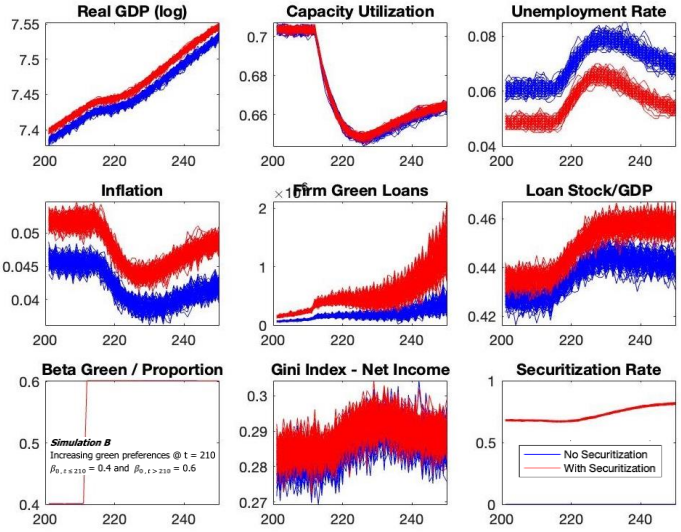

Conclusions. The introduction of differentiated green and conventional securitization markets can boost green investment but also pose financial stability risks and exacerbate inequality. These findings encourage further research on hybrid policy packages, including the proactive management of risks and the direction of capital toward sustainability. Expanding the toolkit to include additional sustainable finance instruments could enhance resilience and equity. Green securitization is no silver bullet but a key lever for financing an orderly green transition.

References

Botta A, Caverzasi E, & Russo A (2024). Same old song: On the macroeconomic and distributional effects of leaving a Low-Interest Rate Environment. Structural Change and Economic Dynamics 69: 552–570.

Botta A, Caverzasi E, Russo A, Gallegati M, & Stiglitz JE (2021). Inequality and finance in a rent economy. Journal of Economic Behavior and Organization 183: 998–1029.

Dafermos Y, Nikolaidi M, & Galanis G (2017). A stock-flow-fund ecological macroeconomic model. Ecological Economics 131: 191–207.

Double-edged solar geoengineering: Impacts and responses for termination risks

Guo-Liang Zheng, Beijing Institute of Technology, China
Email: glzheng99@foxmail.com
IIASA Mentors: Michael Freiberger (EF) and Stefan Wrzaczek (EF)

Introduction. Rapid global warming has intensified interest in Solar Geoengineering, also known as Solar Radiation Modification (SRM). Unlike indirect cooling strategies that target CO_2, such as carbon emission reductions or carbon dioxide removal, SRM bypasses the carbon cycle inertia, offering a potentially fast and cheap cooling effects. However, SRM does not address the root cause of climate change (GHG accumulation) and may introduce novel risks to human and ecosystems. A particularly critical concern is of termination shock risk, i.e., the catastrophic consequences of a sudden failure or cessation of SRM deployment (Trisos et.al, 2018). This proposal aims to explore the impacts of termination shock risk and to identify the optimal response strategy.

Methodology. We develop a stochastic integrated assessment model (IAM) that endogenizes termination shock, capturing both its dynamic evolution and associated damages. The theoretical analysis reformulates the stochastic IAM into a two-stage optimal control model with stochastic switching (2SOCS), providing clear economic intuition. In parallel, the numerical algorithm for 2SOCS addresses key challenges in solving stochastic IAMs, including the "curse of dimensionality" and "non-stationarity" (Cai, 2019). The numerical results quantify the climate–economic impacts of termination shock and identify the optimal response strategy, combining mitigation and SRM policies.

Results. *Before tipping*, a "myopic" DM, who does not account for the termination shock risk, increases carbon emissions and SRM level substantially relative to the abatement-only scenario, whereas a forward-looking ("smart") DM will actively reduce SRM levels as well as emit less, however still above the abatement-only case. *After tipping*, both myopic and smart DMs will abandon SRM and sharply cut emissions, which fall below abatement-only levels. The savings rates drop abruptly, then recover gradually. Besides, the termination shock triggers rapid warming: 0.4–0.6 °C within five years if mid-century, rising to 0.6–1.2 °C if late-century. Economic output rises slightly pre-tipping but drops sharply upon shock, remaining below abatement-only though output rises gradually after tipping. At the end of the century, the myopic DM yields a net GDP uncertainty range of about 665–807 trillion USD, whereas smart DM narrows it to 754–799 trillion USD, indicating smaller post-shock losses. From expected path perspective, myopic DMs emits 6–10 Gt CO_2 more annually than abatement-only; smart DMs emits 2–3 Gt CO_2 more.

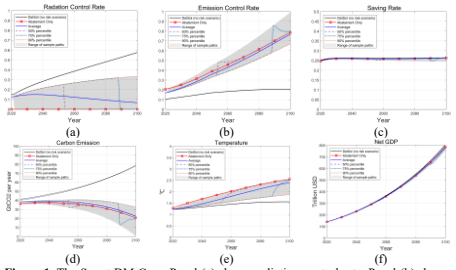

Figure 1. The Smart DM Case. Panel (a) shows radiation control rate. Panel (b) shows emission control rate. Panel (c) shows saving rate. Panel (d) shows annual carbon emissions (Gt CO_2). Panel (e) shows temperature anomaly (°C) (increase in atmospheric temperature above the pre-industrial level). Panel (f) shows net output available for consumption or savings (Trillion USD). In each panel, the red dashed line with mark represents the Abatement-Only solution. The black line represents the solution before tipping under smart decision maker who aware the shock risk. The blue line represents the expected path from the stochastic model. The grey-shaded area shows the range of myopic paths from 10,000 simulations of the optimal stochastic model's solution. The percentile paths measure the tipping probabilities of the shock event at a certain period, as well as the optimal response after the tipping event.

Conclusions. SRM can temporarily offset warming but introduces new risks, notably termination shock. Anticipating this risk enables effective prevention. Smart DMs, who anticipate the risk, emit less pre-tipping and limit GDP losses post-tipping, and better mitigate rapid warming after shock, demonstrating the value of proactive strategies against termination risk.

References

Cai, Y. (2019). Computational methods in environmental and resource economics. Annual Review of Resource Economics, 11, 59-82.
Trisos, C. H., Amatulli, G., Gurevitch, J., Robock, A., Xia, L., & Zambri, B. (2018). Potentially dangerous consequences for biodiversity of solar geoengineering implementation and termination. Nature Ecology & Evolution, 2(3), 475-482.

Energy, Climate, and Environment (ECE)

Exploring the links between Carbon Management Technologies (CMTs) and multidimensional wellbeing in mitigation pathways

Camille Wejnert-Depue, University of Maryland, United States
Email: cwejnert@umd.edu
IIASA Mentors: Elina Brutschin (ECE), and Marina Andrijevic (ECE)

Introduction. Carbon Management Technologies (CMTs), including fossil-based CCS and novel CDR options like BECCS, DACCS, and enhanced weathering, are vital to achieving net-zero emissions targets. While their climate benefits are known, broader wellbeing impacts are less clear. This study examines links between CMT deployment and economic stability, health, and living standards, aiming to integrate wellbeing into climate strategy design and highlight both trade-offs and co-benefits. Their deployment can influence air quality and job creation, which are critical determinants of wellbeing. Yet few studies explicitly connect these technologies to broader social and economic dimensions of climate policy.

Methodology. IPCC AR6 mitigation pathways (C1 – 1.5°C scenarios, C2 – 1.5°C scenarios with overshoot, and C3 – 2°C scenarios) were analyzed at the R10 level using MESSAGE and REMIND outputs. CMTs were categorized as 'Fossil CCS' or 'Novel CDR', linked to net-zero CO_2 target dates. Wellbeing indicators included air pollution mortality and energy-sector jobs. Regression and correlation analyses identified relationships, supported by an R-based integration tool. Comparing multiple models highlights areas of convergence and uncertainty, ensuring results are relevant both globally and regionally.

Results. Fossil CCS was associated with higher air pollution mortality in several regions (see figure 1), suggesting potential health trade-offs when fossil generation continues. Novel CDR results show a positive association with mortality in Europe, India, and North America. Employment outcomes differed: results indicate a positive relationship between fossil CCS deployment and fossil sector jobs, while novel CDR did not provide much of a significant change. Benefits were unevenly distributed, shaped by infrastructure, skills, and economic conditions. These findings emphasize that societal impacts vary across regions, with some benefiting more from CCS and others from novel CDR investments.

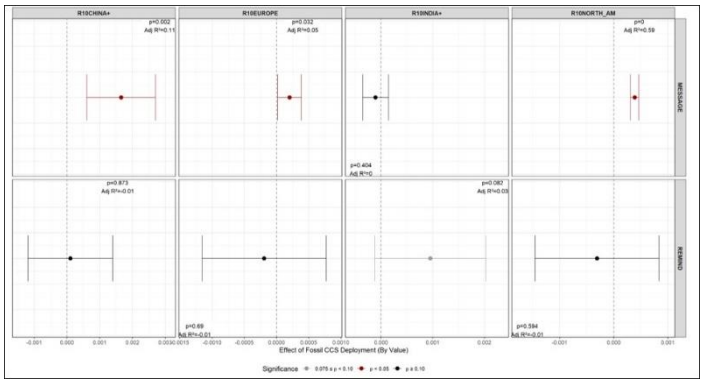

Figure 2. Effect of Fossil CCS Deployment on Air Pollution Mortality

Conclusions. CMT type influences wellbeing outcomes: fossil CCS may sustain jobs but harm health, while novel CDR offers cleaner potential yet uneven benefits. Policymakers should weigh these trade-offs to align mitigation with wellbeing goals. Integrating wellbeing provides a clearer view of pathway trade-offs and helps design climate strategies that not only reduce emissions but also support resilience and opportunity.

References

Chateau, J. & Saint-Martin, A. (2013). *Economic and employment impacts of climate change mitigation policies in OECD: A general-equilibrium perspective.*
Rao, N.D., & Min, J. (2017). *Decent Living Standards: Material prerequisites for human wellbeing*.
Lamb, W.F., & Steinberger, J.K. (2017). *Human Wellbeing and Climate Change Mitigation.*

Producing poverty – Studying the winners and losers of energy provision through the case of Swedish district heating

Jack Vahnberg, Malmö University, RISE Sweden, Sweden
Email: jack.vahnberg@ri.se
IIASA Mentors: Caroline Zimm (ECE), Leila Niamir (ECE), and Luca Casamassima (ECE)

Introduction. District heating is a potentially low-carbon-emission technology for heating (and potentially cooling) a large number of buildings. In Sweden, more than half of the total building stock, 20% of the single-family houses and close to all of the multi-family houses (90%) are heated with district heating. At the same time, district heating has since the 90:ies been deregulated and 41% of the networks have been sold to non-municipal owners. We will use the Swedish district heating market as a case study of how energy provider ownership affects the distribution of resources between households. Is it the case that our energy systems distribute resources so that some households gain at the expense of others?

Methodology. To estimate the distribution of energy burdens, the cost of heating as a share of income, among households, and potential gains such as capital income and assets, we utilize a unique combination of register data. We merge measured energy usage from energy performance certificates with socioeconomic data from tax registries, both on the property level, with price and firm economic data. By studying households living in single-family houses, we are in this way able to estimate household costs directly and associate them with an energy provider. We then complement this data manually through company press releases and ownership registries to see who the final owner of the network is. The result is a panel covering 30% of the single-family housing stock using district heating over the period 2018-2022.

Results. Contrary to the commonly cited belief that energy poverty is close to non-existent in Sweden, we find that around 11% of the households experience large energy burdens (>10% of total income). Crucially, households with large energy burdens have zero to little capital income, indicating that they do not directly profit from private ownership of grids, nor from the private ownership of fuel providers or credit givers (see figure). Diving into the detailed ownership of the district heating networks, 96% of the private networks are owned by four larger companies. These firms have international investors, mostly institutional such as large pension or mutual funds. Finally, taking the perspective of a fair energy burden with equal revenue for providers, we find that if all households shared burdens equally, energy burdens would be around 5% of income, with low-income households paying a lower heating price and high-income households paying a higher one.

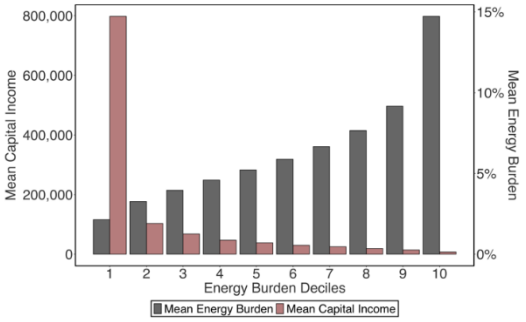

Conclusions. Rather than viewing energy poverty as an isolated issue of a vulnerable population, our research indicates that it is a product of institutional arrangements of energy provision. Specifically, ownership of networks, fuel production and credit givers allow some households to gain at the expense of others. This distributional perspective of energy access puts pricing and ownership at the centre of the analysis, adding to current understanding. At-cost provision would alleviate these issues, and long-term policy makers and civil society could consider heating as a right scheme with low or no costs for households.

Sectoral Emissions Trading in National Energy Systems Model: An Application to Indian Cement and Steel Sectors using MESSAGEix modelling framework

Shreeyash Nitin Malode, Indian Institute of Technology Kanpur (IITK), India
Email: shreeyashmalode@gmail.com
IIASA Mentor: Setu Pelz (ECE), Siddharth Joshi (ECE) and Shonali Pachauri (ECE)

Introduction. Emission Trading Systems (ETS) provide a cost-effective compliance pathway for hard-to-abate sectors, such as cement and steel, which have high marginal abatement costs (MAC). Although Integrated Assessment Models (IAMs) frequently model inter-regional emissions trading, they lack the granularity for intra-regional, cross-sectoral trading dynamics. This study addresses this gap by integrating detailed cross-sectoral allowance trading, into a single-region model.

Methodology. This study employs the MESSAGEix least-cost energy system optimisation framework[1], applied to India's cement and steel sectors by incorporating a portfolio of conventional and decarbonisation technologies. Within this model, ETS is simulated for a single region by applying effort-sharing principles[2]. Three distinct scenarios are evaluated: (1) a baseline without emission intensity targets; (2) a target scenario without trading; and (3) a target scenario with inter-sectoral emissions trading, reflecting the prospective Indian Carbon Market (ICM).

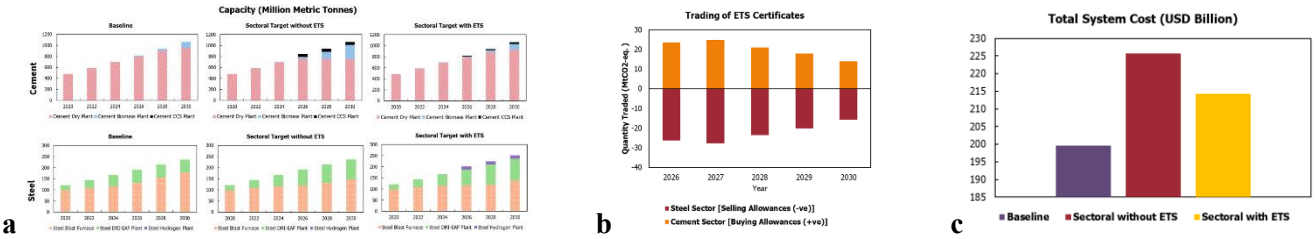

Figure 1. (a) Production capacity by technology, **(b)** trading of allowances, and **(c)** total system cost

Results. The preliminary results indicates that without intervention, greenhouse gas emissions from both the cement and steel sectors are projected to rise. Under the ETS mechanism, the steel sector invests in 14.40 MMT of hydrogen-based production and sells surplus allowances. This enables the cement sector to phase in carbon capture and storage (CCS) to a capacity of 34.28 MMT by 2030. A total of 101 $MtCO_2$-eq. in allowances are traded at a price of USD 61 per tCO_2-eq. This market mechanism reduces the total system cost by approximately 5% relative to the non-trading compliance scenario and lowers total emissions by 10.5% compared to the baseline.

Conclusions. This trading mechanism facilitates cost-effective compliance by enabling the cement sector to finance the steel sector's emission intensity reductions. Implementing this ETS model within MESSAGEix enhances the analytical capability of IAMs and provides a tool to inform national ETS policy regarding technology investments, emission cap trajectories and their impacts on energy system and cost, thereby supporting national carbon budget planning.

References

Huppmann, D., Gidden, M., Fricko, O., Kolp, P., Orthofer, C., Pimmer, M., Kushin, N., Vinca, A., Mastrucci, A., Riahi, K., & Krey, V. (2019). *Environmental Modelling & Software*, *112*, 143–156. doi.org/10.1016/j.envsoft.2018.11.012

Li, M., Pelz, S., Lamboll, R., Wang, C., & Rogelj, J. (2025). *Nature Communications*, *16*(1), 1043. doi.org/10.1038/s41467-025-56397-6

Linking social and environmental impacts within the urban system

Edita Dvořáková, University of Chemistry and Technology (UCT) Prague, Czech Republic
Email: edita.dvorakova@vscht.cz
IIASA Mentors: Benigna Boza-Kiss (ECE) and Shonali Pachauri (ECE)

Introduction. Cities have become major hotspots for environmental and social impacts. If evaluated, urban measures are typically assessed from a one-sided perspective, for example focusing on environmental or economic performance. Social aspects are often considered separately, limiting a systemic understanding of the impacts. However, the interlinkage between social factors and environmental outcomes is evidenced widely, and only anecdotally accounted for in practice. This study bridges quantitative environmental assessment with qualitative system dynamics mapping to holistically evaluate urban measures in Prague, Czech Republic. The approach aims to support planners and policymakers in anticipating trade-offs, managing risks and designing measures that are socially equitable and environmentally effective.

Methodology. The study integrates Causal Loop Diagram (CLD) mapping with consequential Life Cycle Assessment (LCA) to capture both measurable environmental impacts and qualitative social dynamics. Two specific urban interventions - Rohan City Park revitalization and cycling infrastructure expansion - serve as case studies. CLD mapping identifies core feedback loops across social and environmental indicators, validated through a stakeholder workshop. LCA quantifies greenhouse gas emissions, particulate matter and other environmental indicators under different implementation scenarios. For each measure, two LCA scenarios (positive and negative) reflect varying design, maintenance and behavioral responses. Combining these methods allows the identification of leverage points, tests scenarios and highlights unintended consequences that may go unnoticed when assessing environmental or social impacts in silo.

Results. The hybrid CLD-LCA approach shows how measures influence environmental and social outcomes in interconnected ways. LCA results indicate that for cycling infrastructure expansion, the best-case scenario has higher initial environmental impacts due to a construction phase but delivers the greatest long-term benefits through projected behavioral changes. In contrast, the best-case park revitalization scenario consistently yields the lowest GHG and particulate matter impacts throughout its life cycle. CLD mapping in both case studies reveals links between environmental and social factors, with the quality of implementation as a key leverage point. Stakeholder input clarified loop structures and highlighted social thresholds that could shift loops from reinforcing to balancing.

Conclusions. Coupling CLD and LCA offers a more complete picture of urban sustainability measures performance, enabling identification of leverage points, hidden trade-offs, and potential unintended consequences that single-method assessments may miss. The analysis emphasizes that environmental benefits depend not only on technical design but also on conditions and rigorousness of implementation. Inclusive high-quality implementation can initiate reinforcing loops that drive environmental benefits, while ignoring social factors can lock-in long-term negative impacts. Future work could expand to more measures and refine quantitative inputs. Nonetheless, the approach already provides policy-relevant insights for designing interventions that are resilient, socially accepted and beneficial and environmentally effective.

Linking social and environmental impacts within the urban system

Edita Dvořáková, University of Chemistry and Technology (UCT) Prague, Czech Republic
Email: edita.dvorakova@vscht.cz
IIASA Mentors: Benigna Boza-Kiss (ECE) and Shonali Pachauri (ECE)

Introduction. Cities have become major hotspots for environmental and social impacts. If evaluated, urban measures are typically assessed from a one-sided perspective, for example focusing on environmental or economic performance. Social aspects are often considered separately, limiting a systemic understanding of the impacts. However, the interlinkage between social factors and environmental outcomes is evidenced widely, and only anecdotally accounted for in practice. This study bridges quantitative environmental assessment with qualitative system dynamics mapping to holistically evaluate urban measures in Prague, Czech Republic. The approach aims to support planners and policymakers in anticipating trade-offs, managing risks and designing measures that are socially equitable and environmentally effective.

Methodology. The study integrates Causal Loop Diagram (CLD) mapping with consequential Life Cycle Assessment (LCA) to capture both measurable environmental impacts and qualitative social dynamics. Two specific urban interventions - Rohan City Park revitalization and cycling infrastructure expansion - serve as case studies. CLD mapping identifies core feedback loops across social and environmental indicators, validated through a stakeholder workshop. LCA quantifies greenhouse gas emissions, particulate matter and other environmental indicators under different implementation scenarios. For each measure, three LCA scenarios (positive, middle-of-the-road and negative) reflect varying design, maintenance and behavioral responses. Combining these methods allows the identification of leverage points, tests scenarios and highlights unintended consequences that may go unnoticed when assessing environmental or social impacts in silo.

Results. The hybrid CLD-LCA approach shows how measures influence environmental and social outcomes in interconnected ways. LCA results indicate that for cycling infrastructure expansion, the best-case scenario has higher initial environmental impacts due to a construction phase but delivers the greatest long-term benefits through projected behavioral changes. In contrast, the best-case park revitalization scenario consistently yields the lowest GHG and particulate matter impacts throughout its life cycle. CLD mapping in both case studies reveals links between environmental and social factors, with the quality of implementation as a key leverage point. Stakeholder input clarified loop structures and highlighted social thresholds that could shift loops from reinforcing to balancing.

Conclusions. Coupling CLD and LCA offers a more complete picture of urban sustainability measures performance, enabling identification of leverage points, hidden trade-offs, and potential unintended consequences that single-method assessments may miss. The analysis emphasizes that environmental benefits depend not only on technical design but also on conditions and rigorousness of implementation. Inclusive high-quality implementation can initiate reinforcing loops that drive environmental benefits, while ignoring social factors can lock-in long-term negative impacts. Future work could expand to more measures and refine quantitative inputs. Nonetheless, the framework already provides policy-relevant insights for designing interventions that are resilient, socially accepted and beneficial and environmentally effective.

Modeling building stock transitions in a changing climate and energy systems

Shuhaib Nawawi, University of Michigan, U.S.
Email: shuhaib@umich.edu
IIASA Mentor: Alessio Mastrucci (ECE)

Introduction. The residential sector accounts for 20% of U.S. energy-related greenhouse gas emissions, making it central to climate mitigation efforts. However, reducing emissions alone is not enough: 27% of U.S. households face energy insecurity and challenges in maintaining thermal comfort, with low-income families most affected. Climate change will worsen these vulnerabilities through more frequent extreme temperatures. Most models overlook the complex interactions between building stock, climate, and energy systems. This study addresses that gap by analyzing these dynamics at the spatial and temporal scales needed for equity-focused policies.

Methodology. We couple a stock-turnover model (MESSAGEix-Buildings) [1] with a reduced-form building energy model [2]. MESSAGEix-Buildings projects the housing stock required to meet state-level population growth, disaggregated by building archetype and location types (urban, suburban, rural). We scale representative per-area thermal load profiles to projected floor space, yielding hourly thermal demand from 2025 to 2050. We evaluate three demand-side mitigation pathways: REF (business as usual), MOD (moderate retrofits, partial heat-pump adoption, and AGG (rapid deep retrofits, widespread heat pump adoption, urban form shift). Sensitivity analyses address climate uncertainty and alternative grid decarbonization levels.

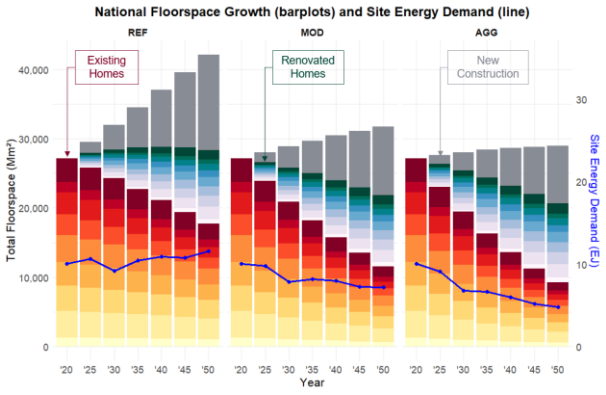

Results. The 2020 baseline reproduces occupied dwelling units within 3% of census totals and aligns national floor space with household surveys, supporting model validity. By 2050, site energy demand diverges sharply across scenarios: +30% in REF, –15% in MOD, and over 50% lower in AGG. The reductions in MOD and AGG stem from deep retrofits, widespread heat-pump adoption, and shift from single- to multi-family homes. The energy mix also transforms: while REF remains ~70% fossil fuels, AGG exceeds 80% electricity. Heating is the main driver of change—rising ~20% in REF but falling 15–20% under MOD and AGG. Cooling grows steadily in REF and MOD, but is stabilized in AGG through efficiency and electrification. Regional patterns vary substantially by state and climate zone, underscoring the importance of tailored retrofit strategies and strong policy support to realize mitigation potential.

Conclusions. Aggressive residential decarbonization through retrofits, electrification, and compact development can greatly reduce energy use and emissions, though impacts differ by region. Ongoing work uses our detailed modeling framework to identify priority areas, assess policy impacts, and guide inclusive energy transition strategies, while also demonstrating its potential to evaluate their effects on household comfort and energy burden.

References

[1] Mastrucci, A., van Ruijven, B., Byers, E., Poblete-Cazenave, M., & Pachauri, S. (2021). Global scenarios of residential heating and cooling energy demand and CO2 emissions. Climatic Change, 168(3), 14.
[2] Nawawi, S., Yi, M., Craig, M., Deetjen, T., & Vaishnav, P. (2025). Cross-sectoral trade-offs in a changing climate: Surrogate models to balance home energy bills, occupant comfort, and power system externalities. iScience, 28(6).

Exploring the indirect energy impacts of digitalised daily life: A test case of smart heating using the FeliX model

Poornima Kumar, University of Oxford, United Kingdom
Email: poornima.kumar@eci.ox.ac.uk
IIASA Mentors: Sibel Eker (ECE) and Quanliang Ye (ECE)

Introduction. Digitalisation is a societal megatrend that already directly contributes 1.8 – 2.8% of global GHG emissions[1]. However, the diffuse indirect energy impacts arising from the social and technological transformations enabled by digitalisation are the true unknowns. These indirect impacts of ICT adoption have not yet been captured comprehensively in many global integrated assessment models. Not accounting for these could result in well-intentioned policy propositions backfiring and inadvertently exacerbating the climate crisis. We develop a module for FeliX, a global system dynamics model, to explore the key feedbacks driving adoption and leading to digital rebound using residential smart heating as a test case.

Methodology. Energy demand in the FeliX model is a function of population and GDP growth rate. We therefore developed a bottom-up module to capture adoption dynamics and energy demand. Stocks of potential adopters (with conventional heaters) and adopters (heat pumps, heat pumps/conventional heaters with smart thermostats) are controlled by adoption and disadoption rates. Adoption is a function of two endogenous feedbacks: technological learning and social learning. As the share of adopters increases, economies of scale drive down the capital cost and risk premium associated with adopting a 'new' technology [2]. Cost attractiveness is shaped by heterogenous implicit discount rates associated with income [3].

Results. We tested low, baseline, and high digitalisation scenarios with different assumptions of (high) implicit discount rate, cost-income threshold, and willingness to adopt heat pumps and smart thermostats. The **high digitalisation** scenario has the highest share of heat pumps and smart thermostats, and hence the lowest relative energy demand.

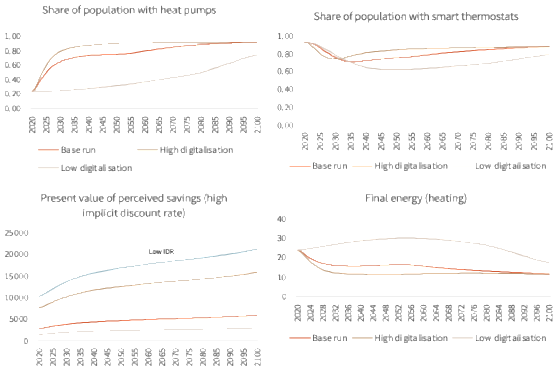

Conclusions. These preliminary findings underscore the importance of accounting for interactions between social and technological learning dynamics. The next steps are to fully endogenise social dynamics with empirical data, explore the social implications of rebound effects, and expand this to cover digitalisation in other residential activities, including technologies such as home energy management systems.

References

Stermieri, L., Kober, T., Schmidt, T. J., McKenna, R. & Panos, E. "Quantifying the implications of behavioral changes induced by digitalization on energy transition: A systematic review of methodological approaches". *Energy Research and Social Science* vol. 97 Preprint at https://doi.org/10.1016/j.erss.2023.102961 (2023).
Edelenbosch, O. Y., McCollum, D. L., Pettifor, H., Wilson, C. & Van Vuuren, D. P. Interactions between social learning and technological learning in electric vehicle futures. *Environmental Research Letters* **13**, 124004 (2018).
Rosenow, J., Barnes, J., Galvin, R., O'Mara, S. & Lowes, R. Total cost of ownership of heat pumps and policy choice: The case of Great Britain. *iScience* **28**, 111784 (2025)

Leveraging temporal and spatial flexibility of renewable-centric data centers in China

Yuezhang He, Tsinghua University, China
Email: heyz21@mails.tsinghua.edu.cn
IIASA Mentors: Bas van Ruijven (ECE) and Xiaoyang Zhong (ECE)

Introduction. Amid accelerating global energy transition, data center (DC)—the backbone of digital infrastructure—are driving rapid growth in electricity demand. By 2030, China's DC are projected to account for about 5% of national electricity consumption. In parallel, China is shifting from fossil fuels to wind and solar, whose intermittency and variability challenge power balance. Integrating data center workloads and renewable deployment thus both stresses grid stability and creates potential flexibility opportunities. DC can shift non-urgent workloads (e.g. AI training) both temporally and spatially to align with renewable generation patterns. Temporal flexibility enables deferral of tasks to periods of high solar or wind output, while spatial flexibility leverages geographically distributed facilities to relocate workloads to regions with surplus renewables or lower electricity prices.

Methodology. This study develops a high-resolution planning–operations framework to assess how temporal and spatial flexibility in data-center loads can reduce system costs, increase renewable utilization, and reshape siting and planning in China. We first project province-level electricity demand under Shared Socioeconomic Pathways (SSPs) and disaggregate workload mixes (rigid/interactive/batch) to construct baseline hourly profiles. We then parameterize temporal flexibility and spatial flexibility via workload migration constraints. Building on these inputs, we develop a province-level, hour-resolution co-optimization model that couples capacity planning and flexible operations for China's DC and renewable energy. Using this high spatiotemporal-resolution model, we quantify system-wide impacts of flexibility strategies on the configuration of DC and renewable resources across SSPs.

Results. We find that surging demand and geographic mismatch make flexibility pivotal. By 2050, DC could account for 5–8% of China's electricity use across SSPs, with the share reaching 31% in Shanghai (SSP2), while regional RE–load mismatches create supply scarcity in load centers. Combining time and space flexibility cuts system cost by 20–27% and CO_2 emissions by 35–60% relative to a Fixed case. Importantly, higher deferrable-workload shares amplify these gains. Even though emission intensity drops by >90% by 2050 without flexibility, the CO_2 trajectories diverge markedly between Fixed and Time+Space, indicating faster and deeper abatement when both dimensions of flexibility are enabled. Flexibility also enhances RE utilization and eases spatial mismatch. By 2050 it raises optimal solar and battery capacity by 50–120% and wind by 5–14%, while reducing required data center peak capacity by ~25%. Sustaining high share of RE-centric data center through 2050 is feasible only when both time and space flexibility are available, which jointly redistribute data center siting and RE build-out and shift workloads from RE-poor to RE-rich provinces.

Conclusions. Data-center flexibility is pivotal for aligning fast-growing digital demand with variable renewables in China. Activating both temporal deferral and interprovincial migration unlocks substantial system benefits: it accelerates emissions abatement, improves renewable utilization, and alleviates regional supply–demand mismatches, enabling durable RE-centric data-center portfolios. These gains persist across alternative socioeconomic pathways, indicating robustness to long-term uncertainty. Practically, flexibility reframes operations—when to run and where to run—rather than simply how much to build. Realizing this potential will hinge on incentives for interprovincial coordination of workload placement, and dependable RE power access, together with measurement and verification practices that make flexible operation transparent and credible.

References

Zhou S, Zhou M, Wu Z, Wang Y, Li G & Wang S (2024). Dual-drive coordinated operation strategy for internet data centers by exploiting spatiotemporal flexibility. Journal of Cleaner Production 450: 141741.
Zhang Y, Li H & Wang S (2025). Decarbonizing data centers through regional bits migration: A comprehensive assessment of China's 'eastern data, Western computing' initiative and its global implications. Applied Energy 392: 126020.

The impact of changes in nitrogen gas emission in climate change mitigation scenarios on air quality in eastern Asia

Koga Yamazaki, Kyoto University, Japan
Email: yamazaki.kouga.78s@st.kyoto-u.ac.jp
IIASA Mentors: Kim Younha (ECE), and Chen Huang (ECE), and Thiago Brito (ECE)

Introduction. Ammonia co-firing is promoted in Japan and South Korea as a decarbonization pathway, but concerns remain over NOx and N_2O emissions. Since these air pollutants contribute to O_3 and $PM_{2.5}$ formation, this study investigates the air pollution impacts of future climate mitigation strategies in East Asia, with a focus on ammonia co-firing.

Methodology. This study applies the Asia-Pacific Integrated Model (AIM) to estimate emissions, downscaled for grid-level GEOS-Chem simulations and provided to GAINS. Air pollutant concentrations are compared between GEOS-Chem and GAINS, while mortality is estimated using Global Burden of Disease (GBD) health impact functions based on pollutant exposure and population data. We analyse three emission scenarios: Baseline, with no restrictions; Mitigation, with stringent reductions to achieve the Paris Agreement's two-degree target; and NH_3, which includes ammonia co-firing. All scenarios are assessed under the SSP2 socio-economic pathway.

Results. In both the Mitigation and NH_3 scenarios, air pollutant emissions were substantially reduced compared to the Baseline. Ammonia co-firing was estimated to occur primarily in the shipping sector (Figure a, b). However, NO_x and NH_3 emissions in the transportation and industrial sectors (due to ammonia production) were higher in the NH_3 scenario than in Mitigation. The average $PM_{2.5}$ concentration estimated by GEOS-Chem was 27.1 μg/m³ in the 2015 Baseline, 16.9 μg/m³ in the 2050 Baseline, 13.0 μg/m³ in Mitigation, and 13.3 μg/m³ in NH_3. The average ozone concentration estimated by GEOS-Chem was 36.9 ppbv in the 2015 Baseline, 37.6 ppbv in the 2050 Baseline, 36.2 ppbv in Mitigation, and 36.9 ppbv in NH_3. The $PM_{2.5}$ concentration difference between NH_3 and Mitigation was estimated to be particularly large in coastal areas with numerous ports (Figure c).

Conclusions. Based on these results, the introduction of ammonia co-firing is suggested to increase ambient $PM_{2.5}$ and ozone concentrations, with the effect particularly pronounced in coastal areas with many ports. Future analyses will present estimates of premature mortality and results from the GAINS model.

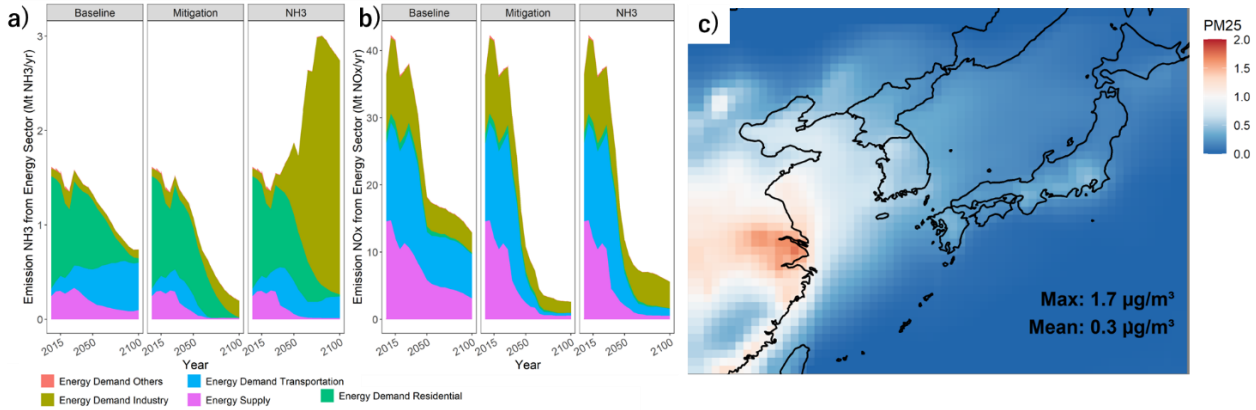

Figure: a) NH3 emissions, b) NOx emissions estimated by sub-sector by AIM. c) Differences between the NH3 scenario and the Mitigation scenario for PM2.5 concentrations by grid in 2050 estimated by GEOS-Chem.

Plant-level decarbonization strategies for power, iron & steel, and cement sectors in China considering health co-benefits

Jianxiang Shen, Tsinghua University, China
Email: shenjx21@mails.tsinghua.edu.cn
IIASA Mentor: Shaohui Zhang (ECE) and Gregor Kiesewetter (ECE)

Introduction. The power, iron & steel, and cement sectors are critical for carbon neutrality due to their substantial climate and health impacts, which account for about 79% of carbon emissions in China, where half of the world's steel and cement are produced. Additionally, China is still facing severe air pollution-related health issues, with near 2 million $PM_{2.5}$-related premature deaths annually, and thus assessing health co-benefits is critical to motivate carbon mitigation actions. However, these sectors face significant challenges: plant-level heterogeneity, complex cross-sectoral resource competition, and material supply and demand. As local policymakers seek detailed transition actions, this study aims to develop integrated plant-level decarbonization strategies for these sectors, incorporating inter-sectoral interactions and health co-benefits.

Methodology. An integrated assessment framework is built. It consists of (1) the Global Change Analysis Model (GCAM)-China for scenario analysis of provincial decarbonization pathways across sectors, especially for power, iron & steel, and cement sectors in Chinese mainland; (2) integrating GCAM-China into Greenhouse Gas - Air Pollution Interactions and Synergies (GAINS) model to explore the health impacts of climate mitigation actions and air pollution control measures; (3) a spatial downscaling method to characterize the integrated layouts of different technologies considering the key material flow across sectors, using plant-level datasets. The key findings from this study can support implementing plant-level mitigation actions in China.

Results. Three carbon mitigation scenarios are developed: a no-climate-policy baseline scenario (REF), a net-zero emission scenario (NZ_limit), and a net-zero emission scenario with enhanced electrification and increased scrap utilization (NZ_circular). Enhancing electrification in the iron & steel (via electric arc furnaces) and cement (via hydrogen-based technologies) sectors achieves an additional 4 EJ reduction in final energy consumption—equivalent to 50% of the savings under the carbon neutrality target. By 2050, carbon neutrality could reduce air pollution by 30~34% and avoid 0.26 million premature deaths in China. In contrast, the strictest end-of-pipe emission control (Maximum Technically Feasible Reductions) in the GAINS model could reduce 47% of air pollution and avoid 0.63 million premature deaths compared to the Current Legislation. The plant-level analysis suggests concrete transition actions in the heavy industrialized provinces: Blast furnaces in southern Hebei should be phased out in the near term, while new scrap-based electric arc furnace plants will mainly be deployed in coastal areas of Hebei and along the Yangtze River in Jiangsu, due to the proximity to the ports or rivers for cheaper transportation costs. Some cement plants in southwestern China would be phased out, whereas most existing cement plants will undergo carbon capture and storage retrofitting to achieve carbon neutrality.

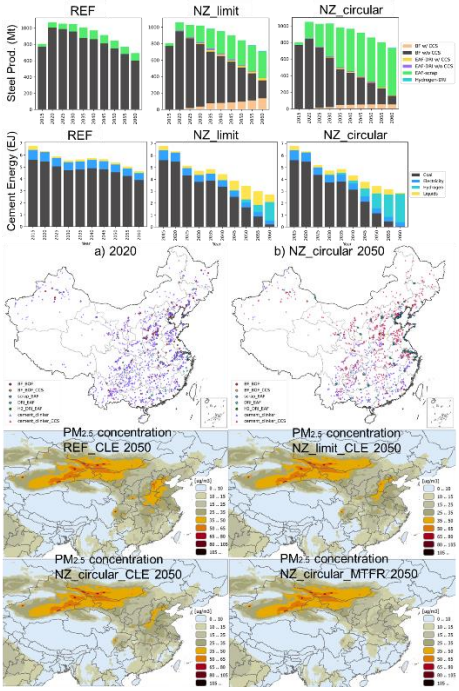

Fig. Steel Production, Cement Energy Use, Iron & Steel Plant Distributions, and $PM_{2.5}$ Concentrations

Conclusions. It is critical to examine the decarbonization pathways of China's power, iron & steel, and cement sectors, and their associated health impacts, through the prism of nuanced spatial dimensions. Our results underscore the necessity of air pollution controls to achieve carbon neutrality, and the significance of spatial heterogeneity in technological attributes and transportation conditions.

The effectiveness of the ASEAN Agreement on transboundary haze pollution

Ji Soo Kim, Korea Advanced Institute of Science and Technology, Republic of Korea
Email: jk1577@kaist.ac.kr
IIASA Mentors: Florian Lindl (ECE) and Zbigniew Klimont (ECE)

Introduction. When environmental challenges cross multiple jurisdictions, addressing them becomes substantially more complex—particularly when political landscapes differ across boundaries. Southeast Asia's recurring haze pollution, driven by climate variability, land-use change, and uneven governance, exemplifies this complexity. In response, the Association of Southeast Asian Nations (ASEAN) introduced an agreement in 2002 aimed at mitigating transboundary haze pollution. Although the ASEAN Agreement on Transboundary Haze Pollution has been subject to legal and policy reviews, its effectiveness has yet to be empirically assessed. This study provides a data-driven evaluation, highlighting how varying institutional capacities shape outcomes across Southeast Asia.

Methodology. This study exploits staggered ratification timing across ASEAN member states to construct a quasi-experimental framework for causal analysis. We employ a quadratic Differences-in-Differences approach combined with a Regression Discontinuity in Time design to estimate the agreement's overall effect on haze levels. The model integrates two decades of satellite-derived haze data with tertiary administrative variables capturing climate (e.g., wind, precipitation), development (e.g., urbanization, forest coverage), and socioeconomic governance conditions.

Results. We find strong causal evidence that the staggered ratification of the ASEAN Agreement on Transboundary Haze Pollution led to a 13-14% reduction in overall haze levels across member states. This effect remains consistently significant across various model specifications and time windows. Spatially, coastal regions—typically more exposed to transboundary pollution—experienced larger reductions (up to 15.4%) than inland areas (as low as 10.6%), indicating effective targeting. Furthermore, effectiveness varies by development level: states with relatively lower development levels recorded the largest reductions (15.1%), followed by those with high (13.5%) and very high (12.7%) levels. Moreover, forest coverage emerges as a key mitigating factor, reinforcing the agreement's emphasis on forest management as a critical mechanism for reducing haze and enhancing policy impact.

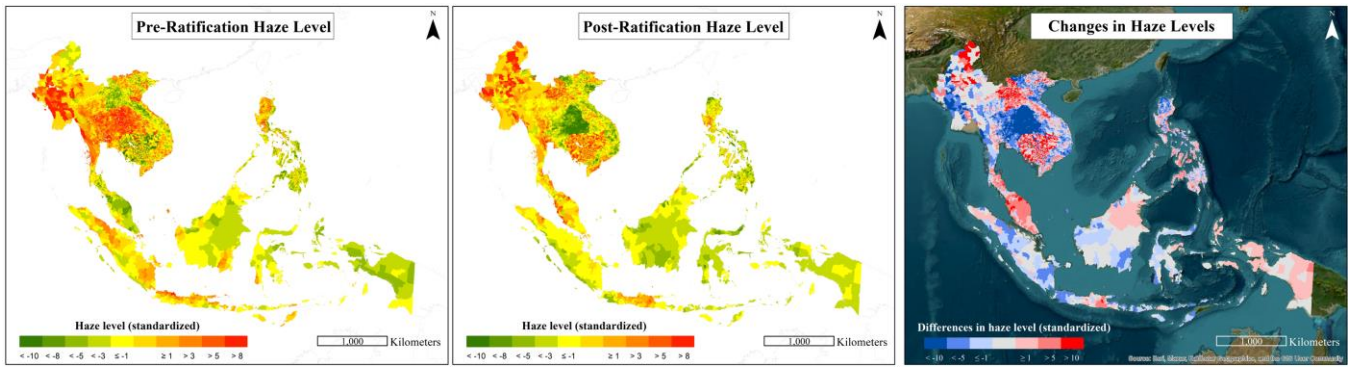

Conclusions. This study demonstrates that multilateral cooperation can effectively reduce transboundary haze, challenging prevailing legal critiques that the agreement's lack of punitive enforcement renders it ineffective. Notably, the extent of effectiveness depends on institutional capacity, shaped by both the pace and maturity of development. These findings underscore the value of flexible, multi-level governance structures that respect diverse sovereignties while addressing complex transboundary environmental challenges.

Assessing Societal Response to Extreme Temperature Shocks

Steffen Lohrey, Technical University Berlin, Germany
Email: steffen.lohrey@campus.tu-berlin.de
IIASA Mentors: Kai Kornhuber (ECE, ICI), and Giacomo Falchetta (ECE, IACC)

Introduction. Future climate projections suggest greatly increased exposure to heat. Recent heat records have been broken by margins that hitherto seemed unlikely. Investigation into physical mechanisms behind these are ongoing, but also the human response to such record-breaking events is important. Insights into societal reactions to such outlier records are important for designing adaptation strategies and to anticipate societal dynamics.

Methodology. We first map heat record margins in recent decades and then merge it with air-conditioning uptake in selected world regions. The analysis is based on heat event indicators from ERA5 and air-conditioning import data from UN Comtrade. We test whether heat records trigger uptake of air-conditioning with both fixed effects methods and event coincidence analysis (ECA).

Results. The occurrence of large temperature records over Europe is spatially heterogenous. For example, parts of France or the UK have experienced record margins beyond 4°C, while larger areas in eastern Europe have not experienced any new temperature records in the past 25 years. A joint analysis of record-breaking years with import value of air-conditioning devices reveals an increased import value following years with heat records in some cases. This observation is currently being tested for its statistical significance and general validity.

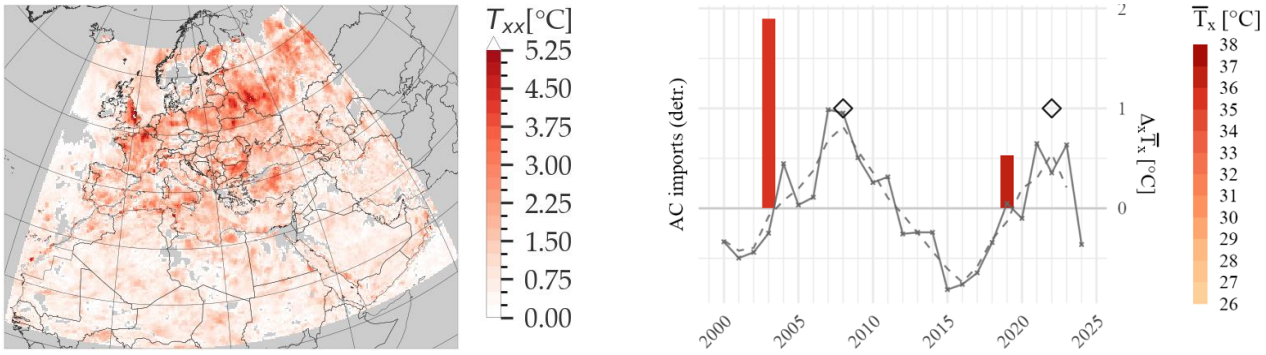

Figure 3: Maximum observed temperature margin to previous record from ERA5 since 2000 (left), record margin and detrended air-conditioning import values with local maxima for France (right).

Conclusions. The statistical significance of record-breaking heat events for peaks in air-conditioning purchasing is being clarified by ECA and fixed effects analysis. The role of further indicators such as number of records can also be investigated. Our research further highlights areas without heat records during the past decades.

References

Falchetta G, De Cian E, Pavanello F & Wing IS (2024). Inequalities in Global Residential Cooling Energy Use to 2050. Nature Communications 15(1): 7874.
Kornhuber K, Bartusek S, Seager R, Schellnhuber HJ & Ting M (2024). Global Emergence of Regional Heatwave Hotspots Outpaces Climate Model Simulations. Proceedings of the National Academy of Sciences 121 (49): e2411258121.
Thompson V, Mitchell D, Hegerl GC, Collins M, Leach NJ & Slingo JM (2023). The Most At-Risk Regions in the World for High-Impact Heatwaves. Nature Communications 14(1): 2152.

Assessing the impact of compound drought-heatwave events on hydroelectric and thermal power generation

Yixu He, Tsinghua University, China
Email: heyixu@iiasa.ac.at
IIASA Mentors: Edward Byers (ECE), Kornhuber Kai (ECE) and Vinca Adriano (ECE)

Introduction. Thermal and hydropower plants, providing over 80% of global electricity(International Energy Agency., 2024), are highly exposed to climate extremes. Compound drought–heatwave events (CDHs) are increasing in frequency and severity, undermining generation efficiency and supply stability(Tripathy et al., 2023). Existing studies largely examine single hazards or specific regions, leaving a gap in global, unit-level understanding of compound risks and technological responses (Wan et al., 2022).

Methodology. Using ISIMIP temperature and discharge data (20 models; historical and SSP1-2.6, SSP3-7.0, SSP5-8.5), we identified global heatwaves, droughts, and compound drought−heatwave events (CDHs). We constructed an enhanced global power plant database, extending WEPP with multiple open sources to integrate cooling technology, dam height, and hydraulic head for 109,110 thermal units and 28,725 hydropower plants. This supported a dual 'mechanism−model' framework quantifying thermal efficiency loss and hydropower reduction, revealing CDH-driven vulnerabilities and regional disparities.

Results. Global thermal and hydropower systems face rising risks from compound drought–heat (CDH) extremes. In 1981–2019, only ~8% of capacity was exposed (~5 days, ~1 event per year), but by 2030–2060 exposure expands to 54–82%, lasting 15–35 days with up to 4 events annually. These extremes put electricity generation at risk of major losses, potentially reaching 1,729 TWh in 2031−2040 (SSP126), with China, the United States, Brazil, and Indonesia most affected. Panels (a) show CDH duration (all plants); (g) maps projected losses.

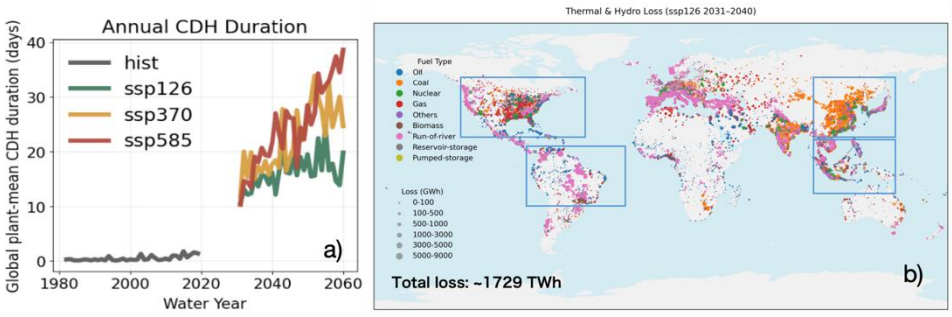

Figure 1. Global CDH duration and associated thermal–hydropower generation losses

Conclusions. Future electricity losses arise not only from more frequent CDH extremes but also from structural fragility—heavy reliance on CDH-sensitive thermal and hydropower, rising demand, and intensifying compound hazards. This "high exposure–high sensitivity–low adaptation" pattern is most pronounced in developing economies, underscoring the urgent need for diversification and adaptive planning in vulnerable power systems.

References

International Energy Agency. (2024). *Electricity 2024.* https://www.iea.org/reports/electricity-2024

Tripathy, K. P., Mukherjee, S., Mishra, A. K., Mann, M. E., & Williams, A. P. (2023). Climate change will accelerate the high-end risk of compound drought and heatwave events. *Proceedings of the National Academy of Sciences*, *120*(28), e2219825120.

Wan, W., Döll, P., & Zheng, H. (2022). Risk of Climate Change for Hydroelectricity Production in China Is Small but Significant Reductions Cannot Be Precluded for More Than a Third of the Installed Capacity. *Water Resources Research*, *58*(8), e2022WR032380.

The role of land and ocean-based geochemical CO_2 removal pathways in climate mitigation

Parisa Javadi, University of Virginia, United States
Email: kcw8qq@virginia.edu
IIASA Mentors: Yoga Pratama (ECE), and Elina Brutschin (ECE)

Introduction. Carbon dioxide removal (CDR) is increasingly recognized as essential for achieving net-zero CO_2 emission targets. We extend the MESSAGEix modelling framework to incorporate two geochemical CDR (GeoCDR) pathways: enhanced rock weathering (ERW) and ocean alkalinity enhancement (OAE). Removal timing and permanence characteristics of GeoCDR are poorly represented in energy models and IAMs; hence, a detailed representation of these factors is implemented.

Methodology. For ERW, we evaluate two silicate feedstocks (basalt and dunite) and varying rock granulometries—reflecting distinct weathering kinetics and slower (basalt) to faster (dunite) removal regimes. OAE is represented via carbonate (limestone) and silicate (dunite) material applied in countries Exclusive Economic Zones (EEZs), with parameterized dissolution rates capturing fast versus slow sequestration trajectories. Both GeoCDR approaches are embedded with spatiotemporally resolved growth rates for global land regions[1] (soil pH, temperature, and cropland availability) and EEZs[2] (temperature, and seawater chemistry), reflecting geographical conditions and logistical constraints.

Results. GeoCDR has limited impacts on the climate until mid-century, but it can contribute to national and regional net-zero emission targets in the second half of the century. Annual CDR via OAE and ERW reaches 5 $GtCO_2$/yr and 3 $GtCO_2$/yr by 2100, respectively. For ERW, although ground rocks in 10 (fastest dissolution rate) to 100 microns are available, the model only deploys grains of 10 microns, in all the regions. Although OAE only gets deployed in the most suitable EEZs of each region, 40% of removal will be using limestone in 2080 and by 2100 dunite will be the dominant material for this GeoCDR.

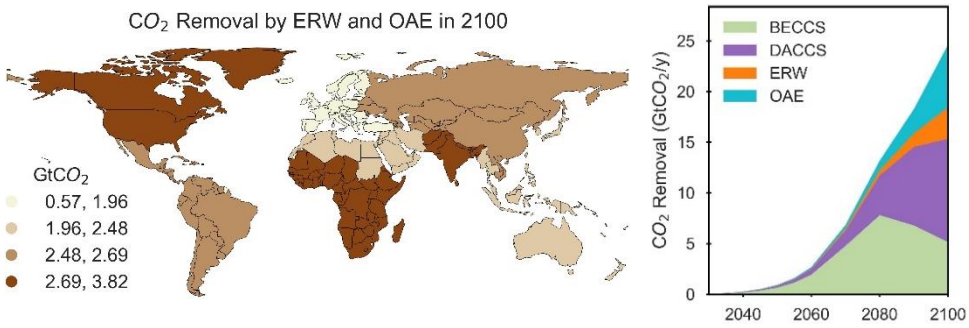

Figure 1. Potential of GeoCDR under SSP2 scenario by 2100

Conclusions. GeoCDR emerges as a critical long-term complement to immediate CDR approaches, offering multi-gigaton potential by 2100. Our analysis highlights that ERW and OAE expand global mitigation portfolios by exploiting abundant geochemical resources, although deployment is highly dependent on dissolution kinetics, regional suitability, and long-term permanence. While their contribution before mid-century seems to be minimal, their scalable role in the second half of the century underscores their importance for sustaining net-zero trajectories.

References

1. Beerling, D. J. et al. (2020). Potential for large-scale CO2 removal via enhanced rock weathering with croplands. Nature 583, 242–248.

2. Zhou, M. et al. (2025). Mapping the global variation in the efficiency of ocean alkalinity enhancement for carbon dioxide removal. Nat Clim Chang 15, 59–65.

Unlocking low-carbon potential: How international climate finance shapes the cost of capital and global decarbonization pathways

Shuting Fan, Tsinghua University, China
Email: fst22@mails.tsinghua.edu.cn
IIASA Mentors: Yiyi Ju (ECE), Adriano Vinca (ECE), and Setu Pelz (ECE)

Introduction. Effective climate change mitigation requires substantial investment, especially in developing economies. Yet high financing costs in many countries remain a key barrier to low-carbon technology deployment. International climate finance (ICF) seeks to alleviate this constraint by providing low-cost capital to unlock low-carbon potential. However, its impact on the cost of capital (CoC) is rarely captured in integrated assessment models (IAMs), limiting understanding of its role in energy transitions. This study integrates ICF and CoC dynamics into the MESSAGEix framework to assess their implications for global and national decarbonization pathways.

Methodology. A country- and technology-specific database of the weighted average cost of capital (WACC) is constructed by differentiating financing structures across renewable and conventional power technologies. Econometric models quantify the historical impact of ICF on WACC and project future WACC trajectories under three scenarios: cwacc (constant WACC), cf_fair_f4 (limited ICF), cf_fair_f10 (large-scale ICF). These dynamic WACC estimates are incorporated into the MESSAGEix model by modifying its investment module to reflect finance-driven cost changes and learning effects, enabling analysis of ICF's role in global decarbonization pathways.

Results. As shown in Fig. 1a, both ICF scenarios (cf_fair_f4 and cf_fair_f10) lead to earlier and larger-scale solar investment. Notably, although the increase in solar deployment under the ICF scenarios is relatively modest, the total investment required is lower, allowing the system to deliver greater clean energy capacity with reduced overall expenditure (Fig. 1c). Under the cf_fair_f10 scenario, total solar investment declines by 1-8% across regions relative to the baseline, with the largest reductions occurring in Sub-Saharan Africa (AFR) and South Asia (SAS). Furthermore, Fig. 1b shows that electricity prices in AFR fall under the ICF scenarios, remaining 0.1-0.8 US$/GJ below the cwacc baseline from 2040 onward and about 0.74 US$/GJ lower by 2100. This reflects the combined effects of reduced financing costs and increased investment in cost-effective solar generation.

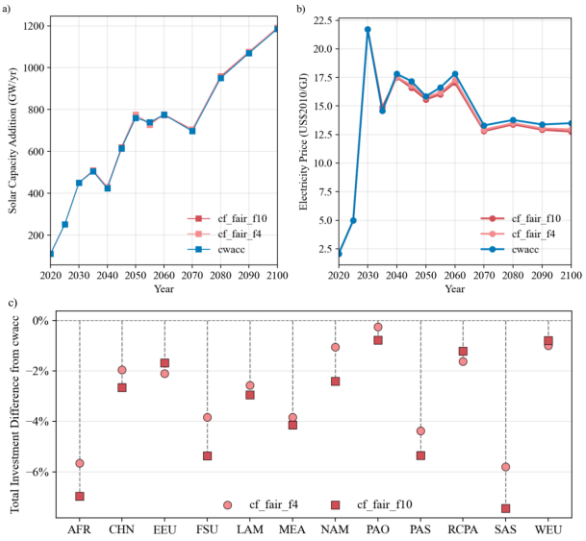

Figure 1. Impacts of international climate finance: (a) solar capacity additions; (b) electricity prices in Sub-Saharan Africa; (c) regional solar investment changes, 2020–2100, relative to baseline.

Conclusions. The results show that ICF improves access to affordable capital across regions, fostering clean energy investment and accelerating deployment. By alleviating financial barriers, it facilitates more efficient deployment of clean energy and improves energy affordability, particularly in capital-constrained regions.

References

Calcaterra, M., Aleluia Reis, L., Fragkos, P., Briera, T., de Boer, H. S., Egli, F., Emmerling, J., Iyer, G., Mittal, S., Polzin, F. H. J., Sanders, M. W. J. L., Schmidt, T. S., Serebriakova, A., Steffen, B., van de Ven, D. J., van Vuuren, D. P., Waidelich, P., & Tavoni, M. (2024). Reducing the cost of capital to finance the energy transition in developing countries. Nature Energy, 1–11.

Multi-model analysis of global hydrogen trade development in a low-carbon energy system

Jana Fakhreddine, University College London, United Kingdom
Email: jana.fakhreddine.22@ucl.ac.uk
IIASA Mentors: Siddharth Joshi, Luca Casamassima, and Volker Krey (ECE)

Introduction. Hydrogen is expected to play a key role in global energy system decarbonisation, with its trade enabling flexible energy transport and storage – unlike electricity. However, the evolution of global hydrogen trade is still uncertain. Associated technical, economic, and political complexities are yet to be comprehensively explored in trade modelling literature[1], despite the burgeoning number of hydrogen strategies[2] and project[3] announced. In this research, we model the dynamics of hydrogen trade development in global low-emission scenarios, examining how current policies and supply developments influence market formation and potential trade patterns.

Methodology. We developed a multi-model scenario analysis approach using two energy system optimisation models, TIAM-UCL and MESSAGEix. We compared hydrogen system representation between models and calibrated for key data points. Seven scenarios were developed: (1) **Ref,** where hydrogen supply was bounded by announced plants reported in the IEA hydrogen production projects database[3]; (2) **High**, where all announced hydrogen projects were assumed to come online. Two variations of these were then developed: (3) **Ref_NT** and (4) **High_NT** with disabled global liquid hydrogen trade; (5) **Ref_TP** and (6) **High_TP** incorporating announced hydrogen trade policy targets[2]; and finally (6) **Base** with neither IEA production limits nor policy targets.

Results. A total of 1–6 EJ of liquid hydrogen was observed to be traded globally across scenarios in 2050, with highest volumes achieved in **TP** scenarios. These trade volumes represent 2–16% of total hydrogen production, indicating that supply is more dispersed and less trade-dependent compared to fossil fuels. Hydrogen trade is seen to facilitate energy system decarbonisation through decreasing total system costs by $6.2–143 billion (between 2020-2100) in the **Ref** and **High** scenarios compared to the **NT** ones. Results show that exporting regions (Australia, South America) produce less hydrogen in **NT** scenarios, while importing regions (Europe, South Asia) produce more expensive hydrogen locally. Results also indicate that hydrogen is expected to contribute to 7-9% of final energy consumption at most, below the 14% estimated by the IEA and IRENA[4].

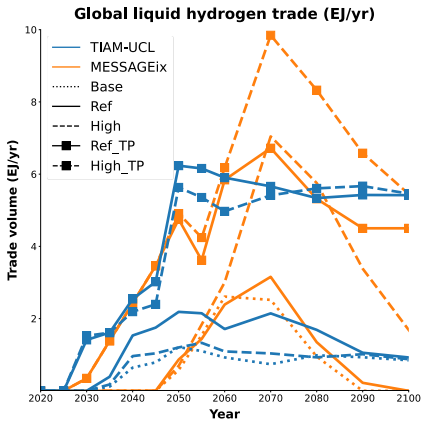

Conclusions. Our findings indicate that global hydrogen trade, despite its limited market size, can facilitate energy system transitions. Benefits of trade are particularly evident for importing regions that gain access to cheap hydrogen imports. The overly optimistic projections in the literature and in policy targets call into question the feasibility of many announced trade goals. Robust modelling that aligns trade expectations with realistic supply, demand, and infrastructure developments will be essential to for a viable global hydrogen trade market evolution.

References

Fakhreddine, J., Dodds, P. E., & Butnar, I. (2025). International Journal of Hydrogen Energy, 129, 236–252.
Corbeau, A.-S., & Nassif, L. (2025). National Hydrogen Strategies and Roadmap Tracker. Center on Global Energy Policy.
IEA. (2024). Hydrogen Production and Infrastructure Projects Database.
IRENA. (2023). World Energy Transitions Outlook 2023: 1.5°C Pathway. International Renewable Energy Agency.

Biodiversity and Natural Resources (BNR)

Developing a global groundwater risk assessment framework

Sara Nazari, Leibniz Centre for Tropical Marine Research (ZMT), Bremen, Germany
Email: sara.nazari@leibniz-zmt.de
IIASA Mentors: Dor Fridman (BNR), and Barbara Willaarts (BNR)

Introduction. Groundwater, a vital component of the global water cycle, sustains ecosystems and provides freshwater supply for billions of people. Yet, increasing dependence, projected to peak around 20501, combined with climate-driven recharge reduction puts these resources at risk. Overuse and depletion threaten ecosystem health and socio-economic stability. Existing global and regional groundwater stress indicators, typically based on withdrawal-to-recharge ratios, have advanced our understanding but remain limited. They often overlook socio-ecological factors and ecosystem needs. In this research, we developed a global groundwater risk framework to address these gaps by integrating human and ecological dimensions and capturing spatial risk patterns worldwide.

Methodology. The groundwater risk framework consists of three components: Hazard, Exposure, and Vulnerability. Hazard is defined as the potential occurrence of natural or human-induced processes that may reduce groundwater availability, quantified using recharge and withdrawal. Exposure reflects the presence of people, livelihoods, or ecosystems at risk, represented by population, groundwater-irrigated areas, and groundwater-dependent ecosystems. Vulnerability captures conditions that increase susceptibility to hazards. Relevant indicators, identified through literature review and expert consultation, were analyzed using Principal Component Analysis to group them into four dimensions, socio-economic, governance, water supply, and ecosystem.

Results. Two types of groundwater risk were evaluated globally, ecosystem risk and societal risk. This report focuses on the latter. The assessment was conducted at a 0.1° grid resolution and aggregated to IPCC regions for policy relevance. Regional outcomes for hazard, exposure, vulnerability, and risk are shown in Figure 1. Results indicate that the most socially vulnerable regions are in Africa. Exposure is highest in densely populated regions such as South and East Asia, while hazard analysis shows that the most extreme conditions occur in the Arabian Peninsula and South Asia. Combining all components, these same regions also emerge as the highest-risk areas. Overall, about two-thirds of the global population live in areas falling within the upper 25% of global societal groundwater risk values.

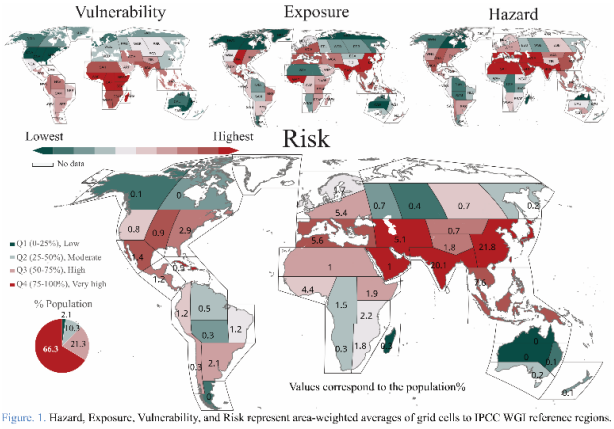

Figure. 1. Hazard, Exposure, Vulnerability, and Risk represent area-weighted averages of grid cells to IPCC WGI reference regions.

Conclusions. This study presents the first global groundwater risk framework, highlighting the combined roles of hazard, exposure, and vulnerability in shaping regional risks. The results show that even in regions with low societal susceptibility, groundwater risk can still be elevated. In contrast, areas like Central and Western-Southern Africa, although classified among the lowest overall risk regions, remain highly vulnerable due to widespread poverty, hunger, and limited access to safe drinking water. These findings emphasize the need to further explore the potential of groundwater resources to improve livelihoods, reduce hunger, and strengthen resilience in such regions.

References

1. Niazi, H., Wild, T. B., Turner, S. W., Graham, N. T., Hejazi, M., Msangi, S., Kim, S., Lamontagne, J. R., & Zhao, M. (2024). Global peak water limit of future groundwater withdrawals. Nature Sustainability, 1-10.

Evaluating the climate resilience of agricultural management practices for improving water quality in Uganda

Gabriel Stecher, BOKU University, Austria
Email: gabriel.stecher@boku.ac.at
IIASA Mentors: Albert Nkwasa (BNR) and Jincheng Li (BNR)

Introduction. In Uganda, 41% of the total land area is affected by degradation. Such degradation, and the associated soil erosion, leads to excessive loss of sediments and nutrients to surface waters, ultimately deteriorating water quality. To combat land and water resource degradation, farmers implement soil and water conservation practices (SWCPs). However, the basin-wide response of surface water quality (Total Suspended Solids - TSS and Total Phosphorus - TP) to SWCPs remains largely unknown, under current and future climatic conditions. The objective of this research is to assess the effectiveness of SWCPs for improving water quality under climate change.

Methodology. To investigate the effects of SWCPs, the Soil and Water Assessment Tool (SWAT) (Arnold et al., 2012) is calibrated and validated for a case study area in Uganda. The major threat to water quality deterioration in the area is poor agricultural land use leading to soil degradation, riverbank erosion and high siltation of water bodies. Field-implemented soil and water conservation practices (SWCPs) (e.g. trenches, mulching, cover crops, etc.) and their application rates (~55%) were identified through stakeholder engagement and outreach, and incorporated into the model. The climate resilience of the SWCPs strategies are assessed by forcing the model with hydro-meteorological data (Gebrechorkos et al., 2022) representing two combinations of socio-economic and representative concentration pathways (SSP2-RCP 4.5 and SSP5 - RCP 8.5).

Results. The hydrological model validation resulted in 16 none-unique parameter combinations with a Kling–Gupta Efficiency (KGE) of > 0.5. TSS and TP were soft calibrated due to limited observations. Forcing the models with four different realizations of each climate change scenario (SSP2-RCP 4.5 and SSP5 - RCP 8.5), water quality is expected to deteriorate further in future. On average TSS increases from 154 mg/L (~2010) to 175-207 mg/L (~2050) and 191-210 mg/L (~2070). TP is likely to increases from 0.21 mg/L (~2010) to 0.22- 0.30 mg/L (~2050) and to 0.24-0.32 mg/L (far future; ~2070). While these results include current SWCP applications, water quality will decline even further without them. The implemented SWCPs have a notable impact on stream water quality, reducing TSS and TP concentrations by 29% and 25%, respectively, during the baseline period. Results suggest that SWCPs remain resilient to climate change and only minor decreases of their effectiveness is expected in future (Figure 1).

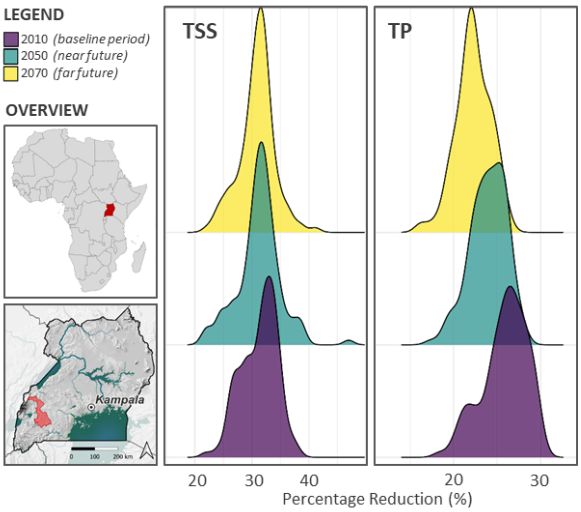

Figure 4: Distribution of TP & TSS reductions for the SSP5-RCP8.5

Conclusions. The strong reduction of TSS and TP highlights the importance of SWCPs to reduce catchment-wide water quality deterioration under climate change. While TSS and TP concentrations are expected to increase considerably in future, the effectiveness of SWCPs remains consistent. However, with current SWCP implementation covering only ~55% of agricultural area, significant expansion of SWCPs will be necessary to offset future climate-driven water quality impacts.

References

Arnold, J. G. *et al.* (2012). SWAT: Model Use, Calibration, and Validation. Transactions of the ASABE, 55(4), 1491–1508.
Gebrechorkos, S.; Leyland, J.; Darby, S.; Parsons, D. (2022): High-resolution daily global climate dataset of BCCAQ statistically downscaled CMIP6 models for the EVOFLOOD project14 December 2022.

Mapping cost-effective adaptation strategies to global quantity- and quality-induced agricultural water scarcity

Weiyi Gu, Peking University, China
Email: weiyi.gu@stu.pku.edu.cn
IIASA Mentors: Taher Kahil (BNR) and Julian Joesph (BNR)

Introduction. Agricultural water scarcity is a critical issue due to its direct impact on food security and cascading effects on economic stability. While previous studies have primarily focused on quantity-induced water scarcity, there is a growing recognition of the importance of considering water quality when assessing water scarcity. Furthermore, although various adaptation strategies have been proposed, there is a lack of systematic economic analysis of adaptation to agricultural water scarcity, particularly in vulnerable basins where water quality is increasingly compromised, making it difficult to identify targeted cost-effective strategies.

Methodology. We integrate quantity- and quality-induced agricultural water scarcity into a unified assessment framework by combining the Global Crop Water Model and the Nitrogen Pollution Model. Socio-economic factors such as population density and agricultural economic dependency are further incorporated to identify the vulnerable basins. We then collect the feasibility, adaptation effects, and economic costs of various adaptation strategies, and conduct a cost-optimization procedure for each vulnerable basin that minimizes the total costs of adaptation subject to various technical and resource constraints. Lastly, we construct Marginal Abatement Cost Curves (MACC) to rank different adaptation strategies based on their respective cost-effectiveness in reducing water scarcity.

Results. Considering only quantity-induced agricultural water scarcity, severe water scarcity (WSI_{quan}>1) occurs in several African river basins, the Indus River, and China's Hai River, due to substantial irrigation water use compounded by relatively limited water availability. When water pollution is additionally taken into account, certain river basins in Europe and North America, as well as China's Yangtze River Basin, emerge as new hotspots (WSI_{qual}>1). Across 275 global river basins, 51 experience severe scarcity when only water quantity is considered (WSI_{quan}>1), but this number increases to 93 once both quantity and quality are included (WSI_{comb}>1), underscoring the critical role of water pollution. We further find that quality-oriented strategies generally yield higher benefits than quantity-oriented ones, with high-frequency, small-dose fertilization showing the highest benefit across the selected basins; In the Hai River, farmers and the society can benefit more than USD 3 per cubic meter of water saved from this strategy. To achieve a 30% reduction in water scarcity in the Hai River, implementing an optimal combination of adaptation strategies could yield benefits of up to USD 5.1 billion.

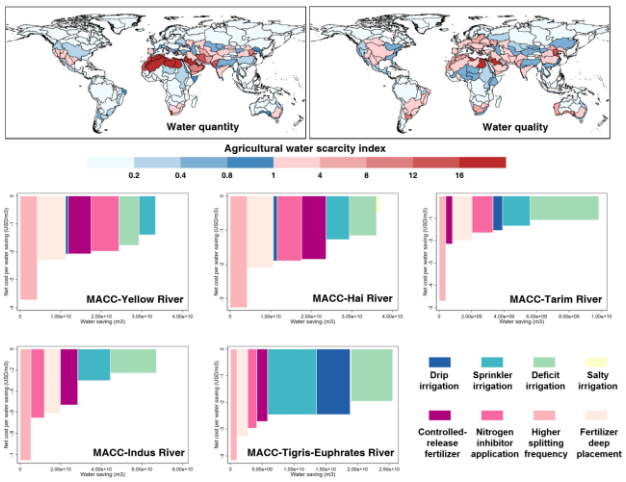

Conclusions. Addressing cost-effectively agricultural water scarcity requires an integrated approach that considers both quantity and quality dimensions alongside socio-economic vulnerability. Our findings show that combining these perspectives enables more precise identification of high-risk basins and the development of tailored adaptation strategies. Quality-oriented strategies, in particular, can deliver substantial co-benefits for both agricultural productivity and environmental health. This integrated framework provides a foundation for designing adaptive water management policies that are both cost-effective and capable of addressing future global water challenges.

References

Baccour, S., Goelema, G., Kahil, T. *et al.* Water quality management could halve future water scarcity cost-effectively in the Pearl River Basin. *Nature Communications* 15, 5669 (2024).

Opening pathways: How infrastructure investment reduces inequality in agricultural adaptation choices

Adham Badawy, Cornell University (USA), NMO: Egypt
Email: ab3263@cornell.edu
IIASA Mentors: Sylvia Tramberend (BNR) and Taher Kahil (BNR)

Introduction. Agricultural resilience under climate change and variability requires a diverse set of adaptation options, yet farmers face systematic constraints limiting adaptive pathways. Contemporary resilience theory emphasizes adaptive capacity in social-ecological systems, yet empirical analysis of how infrastructure access shapes farmers' strategic decisions remains underdeveloped. This research operationalizes Lade et al.'s (2020) pathway diversity framework through developing an agent-based model (ABM) to examine how water infrastructure access affects the management options available to farmers in smallholder agriculture. While measuring resilience has generated extensive literature (Barrett et al., 2021), pathway diversity provides a novel lens for examining individual-level resilience mechanisms. Focusing on Fayoum Governorate's canal irrigation system in Egypt, we investigate how spatial positioning, economic heterogeneity, and infrastructure access produce differential pathway diversity under normal and drought conditions.

Methodology. We develop an ABM featuring heterogeneous farmers differentiated by canal location, farm size, and wealth. Farmers make strategic management decisions regarding water sources, crop portfolios, and infrastructure investments. We introduce a novel archetype-based pathway enumeration approach operationalizing pathway diversity through discrete strategic combinations. Three archetype dimensions are defined: water strategies, crop portfolios, and infrastructure investments. The model integrates satisficing decision-making (Simon, 1956) with behavioral constraints, enabling systematic enumeration of feasible pathway combinations while incorporating quality assessment.

Results. Simulation results reveal systematic pathway diversity inequalities across canal positions and policy scenarios. Under baseline conditions without drought, head farmers maintain 63.9 total pathways compared to 57.3 for tail farmers (gap: 6.6), with effective pathways of 13.7 versus 12.4 respectively (gap: 1.3). Severe drought conditions dramatically amplify these disparities, expanding the total pathway gap to 13.7 and effective pathway gap to 3.3. Collective-only infrastructure policies prove most effective at reducing spatial disparities, achieving near-parity with gaps of only 3.8 total pathways and 0.6 effective pathways under normal conditions. These findings demonstrate that infrastructure access serves as the primary mechanism mediating pathway diversity inequalities, with collective action mechanisms providing more equitable outcomes than individual-focused interventions.

Conclusions. This research advances pathway diversity theory by providing the first systematic implementation within agent-based modeling. The archetype-based approach bridges theoretical concepts with observable farmer strategies, while quality-weighted metrics transform diversity counts toward nuanced adaptation assessment. The satisficing framework provides realistic bounded rationality while remaining computationally efficient for policy analysis. Results suggest collective infrastructure interventions can reduce adaptation inequality while promoting system-wide resilience, highlighting distributive considerations in climate adaptation planning.

References

Barrett CB, Benton TG, Cooper KA, Fanzo J, Gandhi R, Herrero M, James S, Khoury C, Kleinwechter U, Lipper L, Nowak A, Ricciardi V, Rueesch AS, Snowdon W, Yosef S & Zseleczky L (2021). Bundling innovations to transform agri-food systems. Nature Sustainability
Lade S, Haider LJ, Engström G & Schlüter M (2020). Resilience offers escape from trapped thinking on poverty alleviation. Science Advances
Simon HA (1956). Rational choice and the structure of the environment. Psychological Review

Scenarios of dietary transition: Modeling demographic heterogeneity in food demand and nutrient cycles

Avijit Vinayak Pandit, Norwegian Uni of Science and Technology, Norway
Email: avijit.v.pandit@ntnu.no
IIASA Mentors: Marta Kozicka (BNR), Raya Muttarak (POPJUS), and Samir KC (POPJUS)

Introduction. European food systems face transformative challenges requiring evidence-based policy design across demographically diverse populations. Current integrated assessment models (IAMs) employ representative consumer assumptions that obscure critical dietary heterogeneity, particularly demographic differences in food preferences, energy requirements, and waste behaviors. As European policy advances toward sustainable food systems through the Farm to Fork strategy, enhanced modeling frameworks become essential for designing targeted interventions that account for demographic transitions and varying consumption patterns across age, gender, and education groups.

Methodology. We develop a demographic-disaggregated food demand framework that replaces representative consumer assumptions with 54 consumer groups (9 age × 2 sex × 3 education levels) in European contexts. Building on SWITCH Deliverable 7.1 foundations, the methodology implements a four-component demand decomposition: Total Food Energy Demand = Metabolic Need + Overconsumption + Food Waste, with demographic-specific preference multipliers (μ_{ije} coefficients) determining food group allocation. We integrate empirical dietary patterns from the Global Dietary Database (GDD 2018) with metabolic requirements and Physical Activity Level (PAL) categorizations across Shared Socioeconomic Pathway (SSP) scenarios. The framework includes econometric modeling using first-order autoregressive processes with GDP-driven transitions, designed for implementation within GLOBIOM integrated assessment modeling to enable comprehensive scenario analysis.

Results. This work establishes technical infrastructure for demographic-aware food system modeling rather than definitive empirical findings. We demonstrate that 54-group demographic disaggregation produces enhanced demand projections compared to representative consumer approaches while maintaining validation consistency with FAO data sources. The framework incorporates established empirical patterns from European dietary research, including systematic demographic differences in food preferences (higher vegetable consumption among women and older adults, greater meat consumption among men and younger cohorts) and education-related consumption patterns. Integration capabilities enable future quantitative assessment of policy scenarios including plant-based dietary transitions, demographic-targeted waste reduction interventions, and age-specific nutrition programs, providing technical foundations for evaluating multiple sustainable development pathways.

Conclusions. This methodology delivers validated technical infrastructure for next-generation food system modeling in European policy contexts. The framework advances current IAM capabilities by providing (1) demographically explicit demand projections compatible with GLOBIOM integration; (2) component-specific modeling enabling evaluation of targeted interventions; and (3) validated econometric foundations for projecting dietary transitions under alternative socioeconomic scenarios. While quantitative policy assessment requires additional scenario implementation, the methodology enables systematic evaluation of demographic-specific strategies including education-focused interventions, cohort-targeted dietary transitions, and age-differentiated nutrition policies. The framework supports evidence-based evaluation of diverse sustainability pathways, from plant-based dietary shifts to waste reduction programs, providing technical foundations for achieving European Green Deal objectives through demographically-informed food system governance.

References

European Commission (2020). A Farm to Fork Strategy for a fair, healthy and environmentally-friendly food system. COM(2020) 381 final.
KC S, Lutz W (2017). The human core of the shared socioeconomic pathways: Population scenarios by age, sex and level of education for all countries to 2100. Global Environmental Change 42: 181-192.

Disaggregating non-renewable energy use in EU agriculture: An activity-level allocation based on recent econometric modelling

Mamiharimalala Sanda Ny Avo, Université Paris Saclay, France
Email: sanda-ny-avo.mamiharimalala@inrae.fr
IIASA Mentors: Addo Felicity (BNR) and Krisztin Tamas (BNR)

Introduction: Agriculture in the European Union relies heavily on non-renewable energy inputs such as fuels, fertilizers, and electricity, which shape both productivity and environmental outcomes. Rising energy costs and volatility have exposed the structural vulnerabilities of farm systems, yet existing databases and classifications, such as those in FADN, remain too aggregated to capture energy dependencies at the activity level. This research addresses this gap by disaggregating energy use across farming systems, combining econometric modelling with recent advances in allocation methods. The resulting dataset provides a robust foundation for assessing energy intensity, dependency, and resilience in EU agriculture.

Methodology. We use harmonized FADN (2017–2022), ensuring comparability through the standardized construction of utilized agricultural area and harmonized activity groupings. Farms were classified into crop, livestock, and mixed systems using TF14 typology, and acreage shares were derived. A multi-layered preprocessing pipeline was implemented: (i) statistical, multivariate, and density-based outlier detection, (ii) restriction to balanced panels of farms with ≥3 years, and (iii) dimensionality reduction to capture heterogeneity in input structures. Finally, allocation parameters were estimated using a combination of stochastic EM algorithms with Bayesian simulation. Computations were parallelised across 27 EU Member States on IIASA's Limpopo cluster.

Results. Preliminary results focus on the nitrogen allocation in crop systems. The estimation procedure ran successfully for 10 EU countries. Convergence issues in the remaining countries stem primarily from incomplete time series and structural data inconsistencies. For France, the main case study, predicted nitrogen use per hectare exhibits marked crop-specific heterogeneity. Rapeseed and soft wheat show the highest application intensities, while soybean and vegetables remain negligible users. Spatial allocation reveals pronounced regional contrasts, particularly higher nitrogen intensities in northern regions for cereals and oilseeds. Distributional analyses highlight wide within-crop dispersion, confirming substantial farm-level heterogeneity beyond mean values. Temporal profiles indicate relatively stable application levels, with limited downward adjustment despite policy targets.

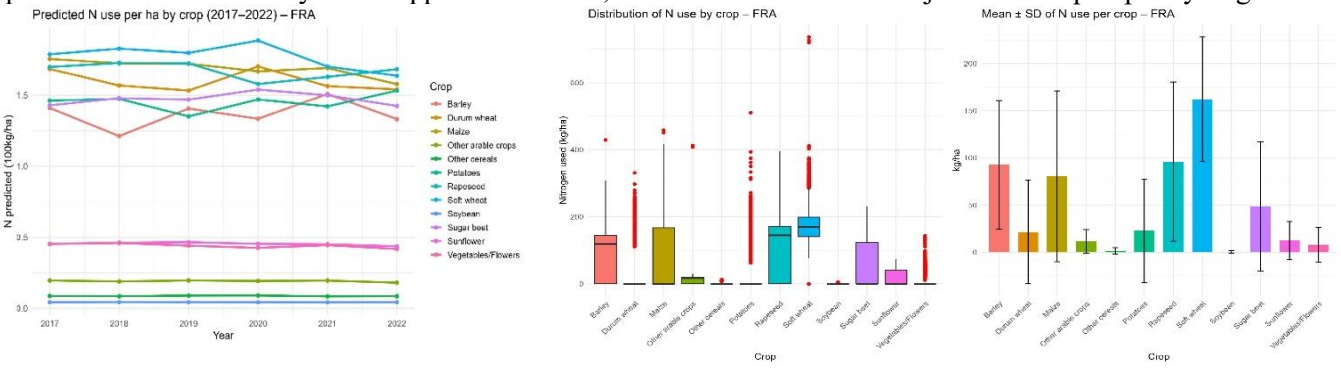

Conclusions. These preliminary results demonstrate the feasibility of activity-level allocation modelling for nitrogen use in crop systems, with robust performance achieved in several EU countries. France serves as a proof-of-concept, highlighting both the strengths of the econometric approach and the limitations due to data gaps. Next steps include extending the framework to livestock and mixed farming systems, and broadening coverage to non-renewable energy inputs such as fuels and electricity. Further harmonization and refinement of outlier treatment will be critical to ensure consistency across countries. Ultimately, the project aims to deliver a disaggregated EU-wide database for policy-relevant energy–environment analysis.

References Koutchadé, O. P., Carpentier, A., & Femenia, F. (2023). Variable Input Allocation Among Crops: A Time-Varying Random Parameters Approach.

Bending the curve 2.0 – Updates on the modelling protocol: note for IAM and BDM modellers

Flavia Aschi, Utrecht University, The Netherlands
Email: f.aschi@uu.nl
IIASA Mentor: David Leclere (BNR)

Introduction. As part of the Kunming-Montreal Global Biodiversity Framework countries have agreed to take urgent action to halt and reverse biodiversity loss. Models and scenarios have been recently used for developing alternative future pathways and explore policy choices to fully reverse biodiversity trends, and the narrative of bending the curve of biodiversity loss gained momentum. Recent work used multi-model ensemble approaches to assess how the trend of biodiversity decline can be reversed by changing future land use or to model the effect of both climate and land-use change across different socio-economic and climate scenarios. The Bending the Curve 2 project (BTC2) aims to go beyond this work by producing ambitious scenarios for reversing biodiversity loss within the 21st century, considering the two main future drivers of biodiversity loss, land use and climate change, and associated policies to mitigate them. This work presents an updated modelling protocol for this exercise, which aims at providing material and implementation guidelines for the Integraded Assessement Modelling (IAMs) teams to generate land use projections for scenarios runs. A schematic representation of the modelling protocol is shown in Figure 1.

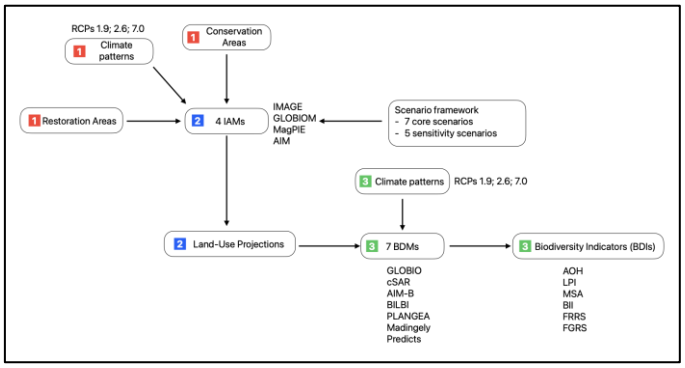

Figure 1. 3-step modelling protocol of BTC2. Part 1 – compiling restoration and conservation layers as well as climate input data. In step 2 - these are input to AIMs for running a set of 12 scenarios. And producing LU projections over different time horizons. Step 3 –LU projections are input for BDMs that will assess the effect of land use and climate change on biodiversity.

Methodology and Results. Conservation and restoration layers and targets were created, alongside guidelines for their implementation by IAMs, decisions for climate change impact and mitigation, and a reporting format for gridded and aggregated IAM outputs. **Conservation target was set to 30% by 2030, following the Global Biodiversity Framework (GBF) target 3. For the gridded layers,** land cover types (Jung et al., 2020) were disentangled from a conservation priority map to produce on a 0.5° × 0.5° grid global maps by land cover type based on a hybrid Level 1-2 IUCN legend. For land cover, the share of pixel area protected and non-protected in 2020, as well as the share proposed to be protected in 2030, were calculated. **Restoration targets** were set to 30% by 2030 and 50% by 2050, following the target GBF target 2. These were expressed as the absolute (Mha) and relative amount of agricultural land considered as degraded and to be restored - identified using land-cover data (LUH2 v2018h), two land-use datasets (LUH2, Ecoregions), and indigenous land (LandMark 2024) - and defined as high intensity cropland, pasture, and rangeland in non-forest ecosystems, and rangeland in forest ecosystems, outside of indigenous land. This spatially explicit data was aggregated at the AgMIP and country level. A 30% target per country was calcuated based on the total degraded land, and compared with FAOSTAT agricultural data to derive the final restoration targets per country. Finally, a survey was circulated to IAM and BDM teams, listing options, interdependencies, and necessary input from all teams.

Conclusions. The results of the survey will allow to refine the modelling protocol to its final version. The aim is to use these results to write a modelling protocol paper to be published on a scientific peer-reviewed journal. Previous examples of such efforts already exist. Although the full ensemble results for BTC2 will be produced in a subsequent research phase, this work establishes a methodological foundation for the rest of the analysis.

References

Jung, M., Dahal, P. R., Butchart, S. H. M., Donald, P. F., De Lamo, X., Lesiv, M., Kapos, V., Rondinini, C., & Visconti, P. (2020). A global map of terrestrial habitat types. Scientific Data, 7(1), Article 1. https://doi.org/10.1038/s41597-020-00599-8

Diagnosing declines in marine biodiversity

Terrance Wang, University of Washington, USA
Email: twangs@uw.edu
IIASA Mentors: Richard Cornford (BNR) and Martin Jung (BNR)

Introduction. Historical declines in marine megafauna have prompted urgent calls to bend the curve of marine biodiversity loss. Designing conservation actions that effectively rebuild species of concern towards intended goals hinges on identifying the key contemporary threats to these species. However, our knowledge of threats to marine megafauna abundances are largely based on expert opinion, thus a more rigorous understanding of the relative impacts of threats on marine biodiversity is warranted. Here, I quantify the impacts of fishing, climate change, urban development, and protected areas on the abundance trends of marine megafauna (e.g., whales, pinnipeds, sea turtles, sharks) at a global scale.

Methods. I first compile a database of population abundances for cetaceans, pinnipeds, sea turtles, and sharks using systematic literature review and other global biodiversity databases, resulting in 772 population time series across 49 species. I hypothesize several drivers that impact abundance: fishing effort, urban development (for land-breeding species), protected areas, and climate change. For each population, I create annual time series of exposure to the drivers by finding the yearly weighted mean of global raster datasets based on spatial weights calculated as a multiplication of the range, habitat suitability model, and dispersal distance decay from survey coordinates. I relate the changes in abundance to exogenous 1-year lagged drivers using a Bayesian multivariate state-space model, that also accounts of endogenous density dependence population growth. I then calculate counterfactual time series for each population by setting these drivers to baseline values (1950-1980).

Results. Climate change has the most prominent negative impact on marine megafauna abundances. Fishing effort and urban development do not have detectable impacts on abundances, as sparse biodiversity monitoring coverage across time, space, and taxa dimensions limited identification of multiple simultaneous external drivers on abundance. Intrinsic population has the largest driving force of population growth. Observed trends show that all major taxa groups are rebounding successfully from historical lows, except for leatherback sea turtles. Counterfactual abundances assuming no climate change has occurred would have led to 0.6x, 2.3x, 1.2x, 1.2x and 1.8x present day abundances for hard-shelled sea turtles, leatherback turtles, eared seals, true seals, and whales, respectively (Fig. 1).

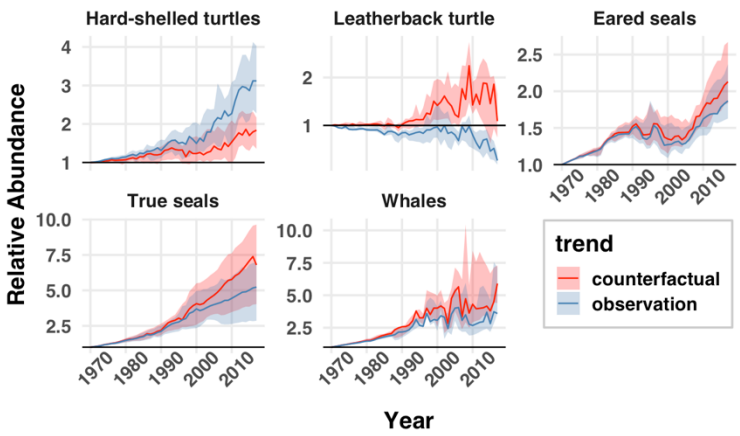

Figure 1. The average trend in abundance relative to 1970 for the 5 major taxa groups colored by observations and counterfactual, where there temperature it set to a baseline period.

Conclusion. Though threats to marine biodiversity have general global patterns, there is still considerable variation in their importance across taxa, space, and time, emphasizing the need for conservation efforts that are context specific. Our ranking of threat impacts by taxa may assist the distribution of limited conservation resources to high priority threats. Counterfactual estimates can facilitate establishing baselines for conservation and management goals for the recovery of the marine megafauna

References

Lewison, R. L., Johnson, A. F., & Verutes, G. M. (2018). Embracing complexity and complexity-awareness in marine megafauna conservation and research. Frontiers in Marine Science, 5, 207.

Are global protected areas effective? Evidence from counterfactual matching of camera trap data

Junjie Liu, Guangxi University, China
Email: hanks_liujunjie@163.com
IIASA Mentor: Martin Jung (BNR), Louise O'Connor (BNR), and Piero Visconti (BNR)

Introduction. Protected areas (PAs) are the cornerstones of global conservation strategies, serving to safeguard habitat integrity and maintain biodiversity. Previous research demonstrates that well-managed PAs can reduce habitat conversion and enhance animal diversity both within protected boundaries and in adjacent unprotected areas. However, many PAs continue to face significant human pressures, leading to habitat degradation, declines in biodiversity, and reduced food web complexity. Thus, further research is required to assess the effectiveness of global PAs in safeguarding wildlife communities and food web networks, as well as to identify the factors that enhance their effectiveness.

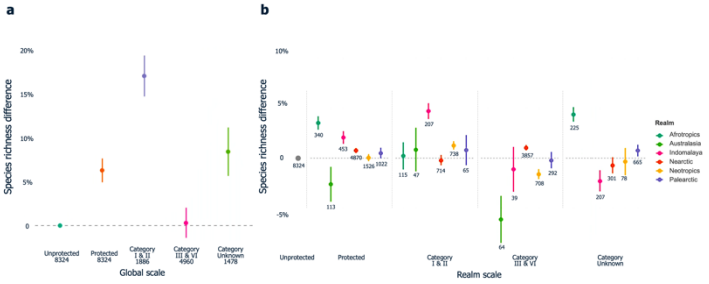

Figure 1. Differences in species richness between protected areas and unprotected sites at global and realm scales.

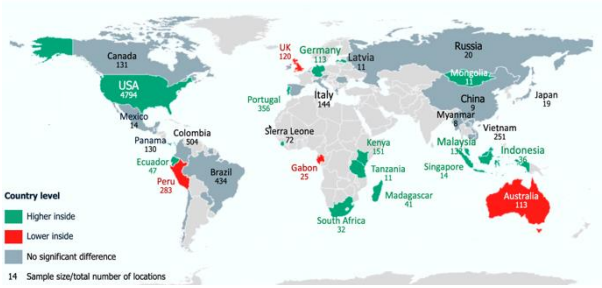

Figure 2. Differences in species richness between protected areas and unprotected sites at the country scale.

Methodology. We compiled a global camera trap dataset from Wildlife Insights (Ahumada et al. 2019) to evaluate the effectiveness of PAs in conserving biodiversity and maintaining food webs. We calculated species richness and food web metrics to estimate protection effectiveness to examine how these effects vary across continents and countries. To account for the non-random distribution of PAs, we applied counterfactual analysis using Propensity Score Matching to pair sites inside and outside PAs, ensuring comparability except for protection status. We then employed a matched-case regression model to assess the efficacy of protection and to examine the impacts of socioeconomic and management circumstances.

Results. Our matched camera trap dataset comprised 8,324 paired protected and unprotected sites, spanning 45 countries, 6 biogeographic realms, and 14 terrestrial biomes. Samples from protected sites exhibited significantly higher species richness than those from matched unprotected sites (Fig. 1a). This effect varied across both regions and countries. At the realm scale, Afrotropic, Indomalaya, and Nearctic showed significantly higher species richness inside PAs than in unprotected sites (Fig. 1b). Australasia contained lower species richness, while the Neotropics and Palearctic showed no significant differences. At the country scale, 14 countries showed higher species richness in PAs, 4 showed lower richness, and 29 showed no significant differences between protected and unprotected sites (Fig. 2). Strict and mixed management categories and total camera working days were positively associated with conservation effectiveness, whereas higher Human Development Index had negative impacts.

Conclusions. Our results highlight that global PAs support higher biodiversity within their boundaries compared to matched unprotected sites. This finding is consistent with previous research showing that global PAs can effectively conserve biodiversity, even without applying strict counterfactual matching. Our results further indicate that strict management enhances conservation outcomes, whereas less strict management does not. Thus, strengthening the management of global PAs is essential. However, these effects varied across regions and countries. Management practices and socioeconomic conditions disproportionately influenced conservation effectiveness. These results suggest that conservation strategies should be tailored to the specific contexts of different countries and regions to maximize effectiveness.

References Ahumada JA, Fegraus E, Birch T, Flores N, Kays R, O'Brien TG & Dancer A (2020). Environmental Conservation 47: 1-6.

Designing nature-positive pathways for Europe's people and biodiversity

Tom X. Hackbarth, Vrije Universiteit Amsterdam, The Netherlands
Email: t.x.hackbarth@vu.nl
IIASA Mentors: Louise O'Connor (BNR), Martin Jung (BNR) and Piero Visconti (BNR)

Introduction. Land use (LU) change, has so far exerted strong pressure on European biodiversity (Hermoso et al., 2022). To counter this, the European Union's (EU) 2030 biodiversity strategy aims to protect at least 30% of EU land (Hermoso et al., (2022). Yet, it is unclear how these policies can be implemented across European landscapes. Here, we develop a range of nature-positive scenarios of LU change in Europe that can support these conservation objectives, halt biodiversity loss and enhance nature's contributions to people (NCPs).

Methodology. We spatially optimized both nature conservation and LU allocation. Starting from SSP1 as a baseline scenario, we translated Nature Futures Framework (NFF) narratives into three alternative LU change scenarios 1) Nature for Nature (N4N) focused on the conservation of species and large, coherent habitats through a land sparing approach; 2) Nature for Society (N4S) prioritized ecosystem and species that provide NCP through multifunctional landscapes; 3) Nature as Culture (NaC) prioritized culturally important landscapes and species of cultural importance. This was operationalized through the conservation optimization model *prioritizr* (O'Connor et al., 2021) and the LU change model CLUMondo (Dou et al., 2023).

Results. Nature-positive pathways are primarily driven by restoration of wetlands and primary forests and agricultural deintensification, particularly in NaC and N4S scenarios with hotspots of deintensification in central Europe. While N4N demonstrates strong increases in natural landscapes, particularly in the Alps, NaC exhibits only weak responses and an overall decline in naturalness. All scenarios reduce landscape heterogeneity to some extent, with N4N displaying the strongest effect.

Conclusions. The NFFs all outline pathways towards a nature positive future for Europe, but each emphasises different values. This study provides guidance for policymakers on how alternative conservation choices may shape European land-use trajectories, and where compromises between different aims will have to be made.

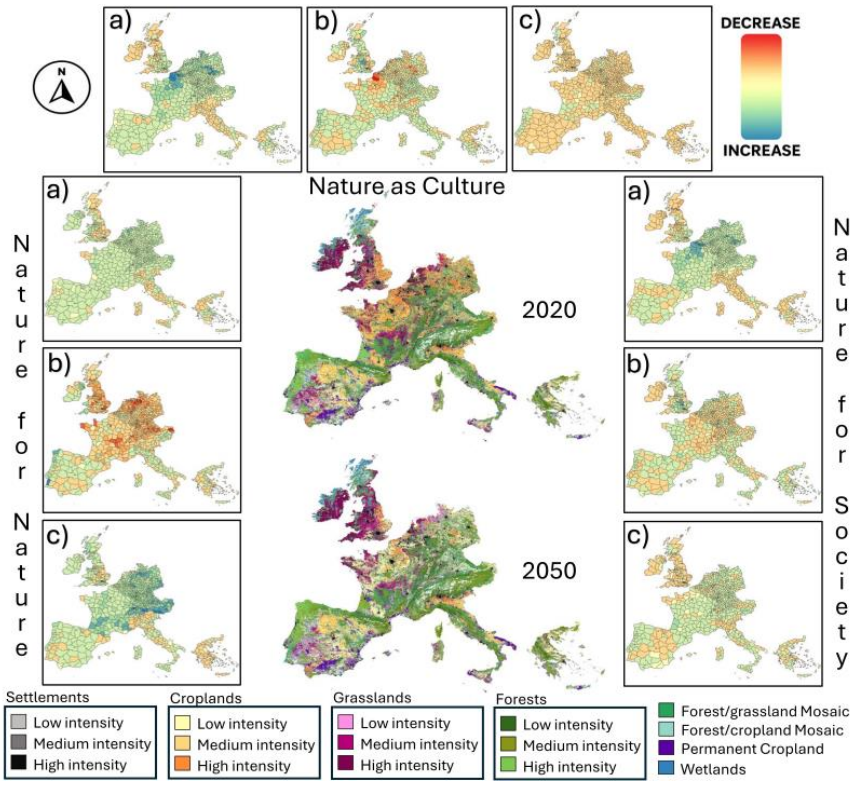

LU change modelling result for Western and Southern Europe. Maps of current European land systems and the baseline LU change scenario are shown in the center. a) Deintensification, b) Diversification and c) Naturalization show trajectories of LU change within the three alternative NFF scenarios.

References

Dou, Y., Zagaria, C., O'Connor, L., Thuiller, W., & Verburg, P. H. (2023). Using the Nature Futures Framework as a lens for developing plural land use scenarios for Europe for 2050. *Global Environmental Change*, *83*, 102766.
Hermoso, V., Carvalho, S. B., Giakoumi, S., Goldsborough, D., Katsanevakis, S., Leontiou, S., & Yates, K. L. (2022). The EU Biodiversity Strategy for 2030: Opportunities and challenges on the path towards biodiversity recovery. *Environmental Science & Policy*, *127*, 263-271.
O'Connor, L. M., Pollock, L. J., Renaud, J., Verhagen, W., Verburg, P. H., Lavorel, S. & Thuiller, W. (2021). Balancing conservation priorities for nature and for people in Europe. *Science*, *372*(6544), 856-860.

Peatland drought resilience in future climate in Europe

Ville Tuominen, University of Helsinki, Finland
Email: ville.tuominen@helsinki.fi
IIASA Mentors: Dmitry Shchepashchenko (BNR) and Juraj Balkovic (BNR)

Introduction. Extreme droughts are a risk to ecosystems, potentially leading to temporal loss of the global land carbon sink (Ke et al., 2024). Peatlands, which are large carbon stock containing twice the amount of carbon found in global wood biomass, may also become annual carbon source during a severe drought year (Rinne et al., 2020). As the number of extreme droughts is expected to increase in the future, there is an increased risk to peatland ecosystems, potentially affecting restoration measures and possibly leading to a climate-warming feedback loop.

Methodology. We simulate peatland sites in Europe using site-calibrated parameters and CMIP 6 climate scenario data. We use process-based peatland ecosystem model JSBACH-HIMMELI, which is based on the JSBACH 3 land ecosystem model combined with the YASSO soil carbon model and the HIMMELI methane transport model. The site-specific model parameters are set by in-situ measurements of greenhouse gas fluxes, water table depth, and weather data. When such data are not available, we have used Sentinel 2 -based maximum Leaf Area Index and a default set of parameters. From CMIP 6, we utilize the MPI and IPSL climate models under RCP 2.6 and 8.5 scenarios.

Results. Drought events, defined by the SPEI drought index threshold of 1990-2020, are increasing especially in the RCP8.5 scenario, where the average number of extreme drought weeks in a year increases by 1.3 weeks. The simulated NEE extremes, however, increase by 3.7 compared to the reference period. In RCP 2.6, the corresponding values are 0.9 and 1.0 weeks. On annual level, interannual variability increases, while only a few sites show statistically significant trends on mean, even under RCP 8.5. Methane emissions, however, are increasing throughout Europe, leading to increased Radiative Forcing of the peatlands. Using different forcing data products, we found also that a past extreme drought is shown in simulation output with less accuracy than an average year.

Conclusions. The calibrated site-simulations using the climate scenario data provide more detailed estimates of how certain types of peatlands react to climate change. There is a clear risk that the peatlands will become more climate warming especially due to the increased methane emissions. The more variable climate leads to more variability of carbon uptake and release, especially in the RCP 8.5 scenario. The model has limited functionality in representing vegetation changes and does not show past extremes in their full extent, meaning the simulated estimates likely underestimate the effect of droughts in future climate.

References

Ke, P., Ciais, P., ..., Chevallier, F. (2024). Low latency carbon budget analysis reveals a large decline of the land carbon sink in 2023. National Science Review, 11(12), nwae367. https://doi.org/10.1093/nsr/nwae367
Rinne, J., Tuovinen, J.-P., ..., Nilsson, M. B. (2020). Effect of the 2018 European drought on methane and carbon dioxide exchange of northern mire ecosystems. Philosophical Transactions of the Royal Society B: Biological Sciences, 375(1810), 20190517. https://doi.org/10.1098/rstb.2019.0517

Modeling the influence of grazing on regional wildfire dynamics in Europe

Rasheed Akinleye Hammed, The University of Manchester, UK
Email: hammedrasheedakinleye@gmail.com
IIASA Mentors: Andrey Krasovskiy (BNR) and Hyun-Woo Jo (BNR)

Introduction. Wildfires has been posing a significant threats to European landscapes and ecosystems. Factors such as climate change, coupled with the rise in human settlements, is expected to intensify, prolong fire seasons, especially across Mediterranean and continental areas of Europe. As part of ongoing efforts to reduce wildfire risk, targeted livestock grazing is increasingly being adopted as an effective fire management strategy (Lovreglio et al., 2024). This study seeks to explore the effects of grazing as an adaptation option at the European, regional and national scales using wildfire model FLAM.

Methodology. Grazing data from Malek et al., (2024) and burned area outputs simulated by FLAM model (www.iiasa.ac.at/flam), were integrated to assess the influence of grazing on wildfire dynamics. Two ratios were first calculated: grazing area to total area (R_1) and burned area in grazed locations to total burned area (R_2). If grazing is ineffective, $R_2 \approx R_1$; $R_2 < R_1$ indicates reduced burning in grazed locations. To capture grazing impacts, we compute the rate of grazing effect (γ), which estimates potential wildfire reduction due to grazing. After assessment of regional grazing impacts, we conduct scenarios for expansion of grazing areas around current locations by factors $f \in (1.25, 1.5, 1.75, 2)$. This approach can be applied at various scales which help identifying locations where grazing is an efficient tool for fire reduction.

Results. Our assessment for entire EU-27 land found that the burned area reduction by grazing was not significant (γ = 0.03). The results are likely influenced by the extensive coverage and broad aggregation of data, which can mask more localized impacts. At national scale, however, scenario analysis shows that expanding grazing coverage lowers burned area by 33% in Spain (γ = 0.33). Using the nationally acquired γ, we simulated the expansion of grazing cover with multiple factors (f = 1.25–2, see figure below). When doubling the grazing area ($f = 2$), burned areas has effectively reduced over 9000 ha on average (see table, right panel). The impacts of grazing are more significant at finer geographic scales compared to broader assessments.

f	Total grazing area (ha)	Increase in total grazing area (ha)	R_1^A	R_2^A	$GrazingBA_1$ (ha)	$GrazingBA_2$ (ha)	$\Delta Grazing^A$ (ha)
1	8,209,442	0	0.156	0.104	14,342.13	14,342.13	0
1.25	10,171,984	1,962,542	0.193	0.129	17,899.60	11,900.00	5,999.61
1.5	11,889,672	3,680,230	0.226	0.154	21,347.20	14,192.03	7,155.18
1.75	13,397,201	5,187,759	0.254	0.178	24,633.98	16,377.14	8,256.84
2	14,724,407	6,514,965	0.280	0.201	27,763.99	18,468.03	9,305.96

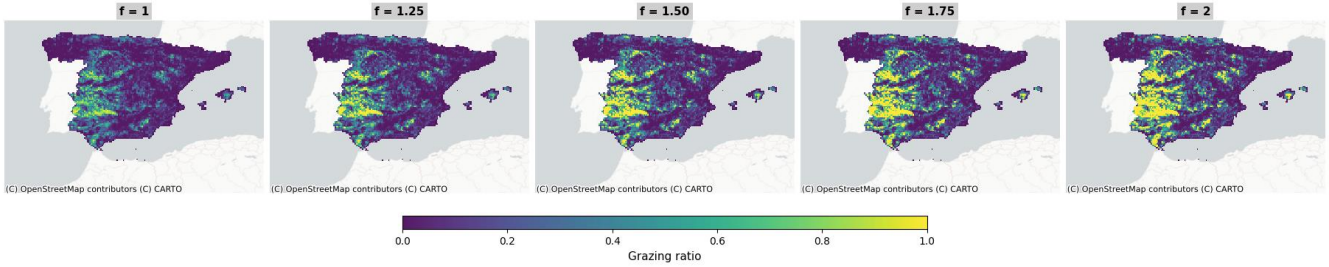

Conclusions. Our analysis indicates that grazing yields substantial reductions at national scales, notably in Spain. More importantly, expansion of grazing coverage as one of the effective adaptation strategies could help mitigate the risk of wildfires in fire-prone regions, particularly across diverse landscapes and ecosystems of Mediterranean countries in Europe (i.e., France, Greece, Italy, Portugal and Spain). However, further research is required to evaluate how impacts of grazing will influence reductions in burned areas under varying climate scenarios.

References

Lovreglio, R., Lovreglio, J., Satta, G. G. A., Mura, M., & Pulina, A. (2024). Assessing the Role of Forest Grazing in Reducing Fire Severity: A Mitigation Strategy. *Fire*, *7*(11), 409. https://doi.org/10.3390/fire7110409

Malek, Ž., Schulze, K., Bartl, H., Keja, W., Petersen, J.-E., Tieskens, K., Jones, G., & Verburg, P. H. (2024). Mapping livestock grazing in semi-natural areas in the European Union and United Kingdom. *Landscape Ecology*, *39*(2), 31. https://doi.org/10.1007/s10980-024-01810-6

From fields to future: A machine learning framework for sustainable carbon and nitrogen management in pan-European agriculture

Bin Du, Beijing Normal University, China
Email: dubinchn@gmail.com
IIASA Mentors: Rastislav Skalsky (AFE) and Thomas Oberleitner (AFE)

Introduction. Food security and agricultural sustainability face the dual challenges of climate change and population growth. In Europe, long-term intensification has increased crop yields, yet excessive tillage and fertilizer overuse have led to soil organic carbon (SOC) depletion, nitrogen (N) surplus, reduced water-use efficiency, and other environmental concerns. The European Green Deal advocates sustainable, climate-friendly practices—such as optimized N fertilization and straw return—to promote both food production and soil health. This study develops an integrated framework combining the gridded Environmental Policy Integrated Climate Model (EPIC-IIASA GAM) with machine learning to support multi-objective co-management at the regional scale.

Methodology. Outputs from the EPIC-IIASA dynamic C–N simulations for 1980–2019 were used, with 86,000 simulation units (SimUs) divided into 12 environmental stratification (EnS) zones. On this basis, the eXtreme Gradient Boosting (XGBoost) algorithm was employed to construct meta-models approximating the complex processes represented by EPIC-IIASA. These meta-models were then applied to identify the key drivers of four target variables—crop yield, SOC sequestration, N surplus, and root-zone soil water (SW). Based on these models, a weighted multi-objective optimization was further performed to achieve coordinated improvements across the four targets and to derive region-specific optimal C–N input strategies.

Results. Overall, SOC sequestration and crop yield are predominantly regulated by management practices, whereas N surplus and soil water dynamics are primarily driven by climatic and soil conditions, with pronounced regional heterogeneity. For SOC sequestration, straw C input is the most important driver. Crop yield is most strongly increased by more N and straw C inputs. N surplus is primarily determined by N fertilization, with additional effects from temperature and initial SOC. Soil water is mainly controlled by climatic and soil properties, with stone content, radiation, silt, and precipitation as the key factors. The optimal C–N management strategies differed across regions and crops. For winter wheat, the optimal C and N inputs were around 4,000 kg ha^{-1} and 200 kg ha^{-1}, respectively.

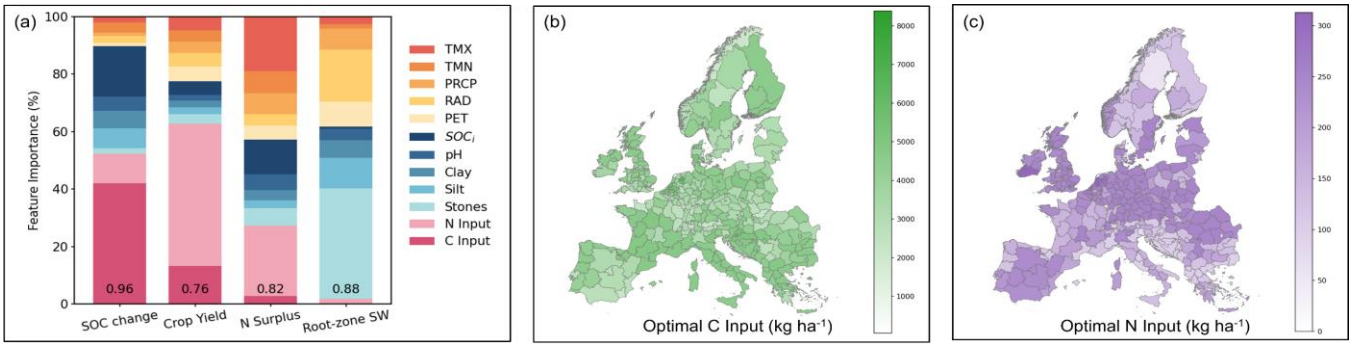

Figure 1. XGBoost feature importance (a) and optimal C and N inputs across pan- European regions (b–c) for winter wheat.

Conclusions. We developed a data-driven modelling framework that simplifies the application of process-based agricultural models and has strong scalability. It is applicable to carbon–nitrogen optimization in Europe and provides a reference for sustainable agriculture and climate change adaptation globally.

References. Ippolito T, et al. (2023). Journal of Environmental Management, 344, 118532.

The role of forestry biomass in the emerging fossil free iron and steel making process

Jim Allansson, Luleå University of Technology, Sweden
Email: Jim.Allansson@ltu.se
IIASA Mentors: Shubham Tiwari (BNR) and Florian Kraxner (BNR)

Introduction. The iron and steel industry is one of Europe's most greenhouse gas intensive industries. To reduce emissions, the industry is transitioning from the traditional blast furnace basic oxygen furnace (BF-BOF) route to direct reduced iron (DRI) combined with electric arc furnaces (EAF). Nineteen steel mills across ten EU27 countries have announced that they will transition by 2030. By utilising renewable electricity and a non-fossil alternative for the metallurgical coal, the DRI-EAF pathway has the potential to be completely fossil-free. Biochar derived from woody biomass has emerged as a promising substitute for the metallurgical coal. However, uncertainties remain regarding how to source the biomass and to what cost. This work sets out to explore the potential of forestry biomass to supply biochar as a substitute to metallurgical coal in the emerging DRI-EAF production route.

Methodology. To explore the role of forestry biomass, a techno-economic assessment was conducted using the BeWhere model. The forestry biomass availability was derived from the S2Biom project harvest potential estimates, subtracting the current forestry biomass demand to indemnify the surplus. Biomass was converted to biochar in a rotary kiln pyrolysis reactor. The biochar demand was estimated by maintaining a carbon mass-balance in the EAF, accounting for carbon from either scrap, DRI, or directly charged in the furnace. Multiple scenarios with different mixes of scrap-to-DRI ratios were created to show how increased/decreased use of scrap steel influences the supply chain and costs of biochar.

Results. Preliminary results show that the cost of supplying biochar is higher in Sweden and the Netherlands compared to Italy and Spain, primarily due to regional biomass price differences. Increasing scrap use in the EAF reduces overall biochar demand, leading to marginal cost decreases in most countries due to reduced transportation requirements. An exception is Germany, where lower production volumes reduced economies of scale, slightly increasing costs. However, even the lowest cost of supplying biochar for both scenarios was still above the cost of the fossil alternative, excluding emission taxes. If accounting for emission taxes for the fossil alternative, a tax of 85 EUR/tCO_2 would be enough to make domestic biochar production a viable option for all countries.

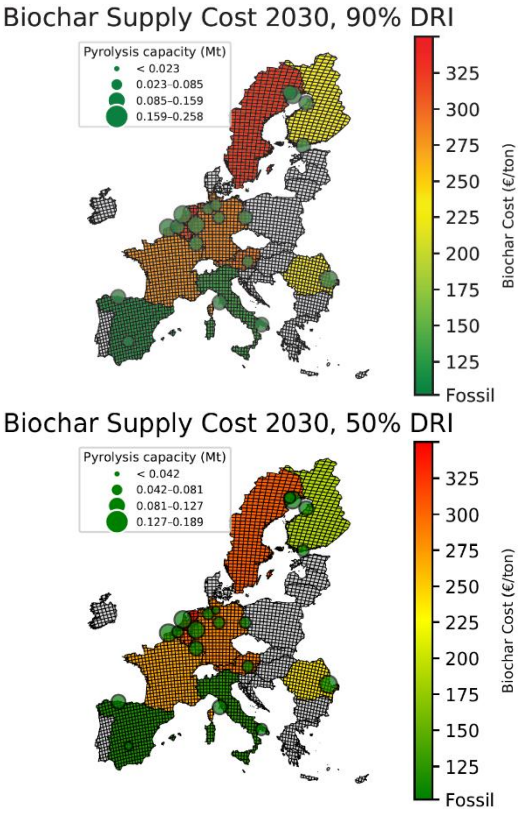

Conclusions. Future carbon demand from the DRI-EAF production route could be met through biochar produced from forestry biomass. However, due to the high cost of biomass, biochar remains uncompetitive to fossil alternatives without further economic incentives. The use of scrap steel has a small impact on the cost of biochar, hence scrap use should be prioritized in regions where DRI production is expensive rather than where biochar costs are high.

Advancing Systems Analysis (ASA)

Algorithmic complexity-based methods for assessing social-ecological resilience

Ross Tieman, Australian National University, Australia
Email: ross.tieman@anu.edu.au
IIASA Mentors: Brian Fath (ASA) and Elena Rovenskaya (ASA)

Introduction. Critical transitions in social-ecological systems can lead to abrupt regime shifts with severe consequences, making Early Warning Signals (EWS) important for adaptive management. While traditional EWS detect statistical changes (variance, autocorrelation) and deep learning approaches identify complex patterns (Bury et al,. 2023), these primarily capture statistical properties of system dynamics. Kolmogorov complexity, approximated through Block Decomposition Method (BDM) (Zenil et al. 2018), offers an alternative lens to view system changes in terms of changes in the sophistication of generative processes capable of producing observed state variable timeseries. Extending work by Dakos & Soler-Toscano (2017), we develop a sliding window approach for online BDM computation, systematically assessing predictive capacity and uniqueness of algorithmic complexity measures against existing EWS.

Methodology. We analyze the five co-dimension-1 bifurcation models under varying noise and forcing conditions. A method for rolling window BDM is developed and computed using three discretizations (mean-based, 5-bin quantiles, first difference). Performance is assessed via Receiver Operating Characteristic (ROC) curves with Kendall's tau at 80% pre-transition timeseries, comparing BDM against variance, lag 1 autocorrelation and deep learning predictors (Bury et al. 2023). Principal Component Analysis is performed on measures to identify dimensional structure of predictive information.

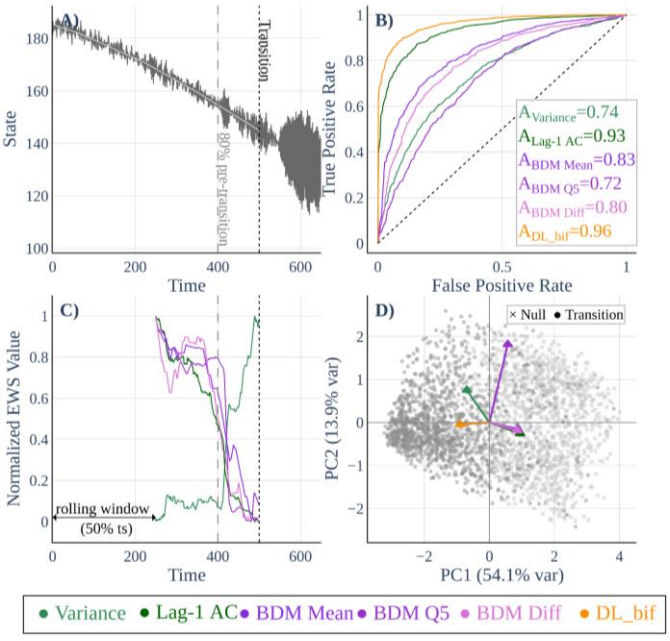

Results. BDM measures achieved Area Under Curve (AUC) of 0.65-0.84 across models, demonstrating capacity to predict critical transitions through algorithmic complexity. Principal Component Analysis revealed BDM loads distinctly on primary predictive components compared to traditional measures. Notably, BDM exhibited bifurcation-specific directional patterns (decreasing complexity in both period-doubling and fold bifurcations despite opposing variance trends), suggesting algorithmic signatures can distinguish transition types.

Conclusions. We establish rolling window BDM as a practical online method complementary to existing early warning signals. The ability to extract predictive information through algorithmic complexity, even in systems optimal for traditional statistical indicators, demonstrates the potential of investigating critical transitions through an algorithmic information dynamics framework. This motivates future work across a wider range of empirical and model systems to establish the value of algorithmic complexity based approaches for SES management where traditional approaches may be limited or algorithmic signatures provide additional insight.

References

Bury T et al. (2023). Deep learning for early warning signals of regime shifts. PNAS 120: e2309838120.
Dakos V & Soler-Toscano F (2017). Measuring complexity to infer changes in the dynamics of ecological systems under stress. Ecological Complexity 32: 144-155.
Zenil H et al. (2018). A decomposition method for global evaluation of Shannon entropy and local estimations of algorithmic complexity. Entropy 20: 605.

Intersectional influences on trust in public health authorities: Insights from a U.S. nationally representative sample

Samantha Kloft, University of Massachusetts Amherst, United States of America
Email: skloft@umass.edu
IIASA Mentor: Jung Hee Hyun (ASA, SI)

Introduction. Amid rising misinformation, political polarization, and declining institutional credibility, trust in public health authorities has become globally strained. Although research on trust has gained attention since 2020, few studies apply an intersectional lens to examine how structural and social forces shape trust across communities. Using the United States as a case study, this project applies the Intersectionality-Based Policy Analysis (IBPA) framework to (1) identify distinct sociodemographic profiles, (2) examine how their trust in public health authorities differs, and (3) analyze how systemic factors and intersecting identities shape these profiles to inform future trust-building policies and practices for more resilient health systems.

Methodology. Data were drawn from the 2024 RAND American Life Panel (N=2,034), a nationally representative survey of U.S. adults. Eight Likert-scale items assessed perceived beneficence to measure trust in public health authorities (CDC, FDA, and local/state officials). Guided by the IBPA framework, which centers power and structural influence on health, this study applied multiple methods from quantitative intersectionality research. Latent class analysis (LCA) first identified sociodemographic trust profiles, followed by descriptive and bivariate tests to compare groups. Then, nested linear regressions sequentially added five substantive domains and tested key interactions. Analyses were unweighted due to LCA software constraints (Stata 18); results reflect internally valid sample patterns rather than population estimates.

Results. Latent Class Analysis supported a three-profile solution (AIC = 53,537.22; BIC = 54,110.23; entropy = 0.708), identifying distinct sociodemographic groups with significantly different trust in public health authorities ($F(2,2031) = 17.86$, $p < 0.001$; Figure 1). Profile 1 (28.1%) included middle-aged, socioeconomically advantaged professionals; Profile 2 (41.4%) comprised older, White retirees with the highest trust ($M = 5.96$); and Profile 3 (30.5%) captured racially diverse adults facing greater structural vulnerability and lowest trust ($M = 5.26$). Nested regressions showed that trust gaps attenuated after adjustment ($F(2,1980) = 1.04$, $p = 0.355$), with socioeconomic status and geography explaining most variance. Interaction models indicated that graduate education predicted higher trust across profiles (e.g., Profile 2: +2.10, $p < 0.001$), but effects varied; in Profile 3, bachelor's degrees were not significant. Life satisfaction increased trust only in Profile 3 ($p = 0.001$), while manual labor, large households, and rural residence predicted lower trust, highlighting uneven benefits of structural resources.

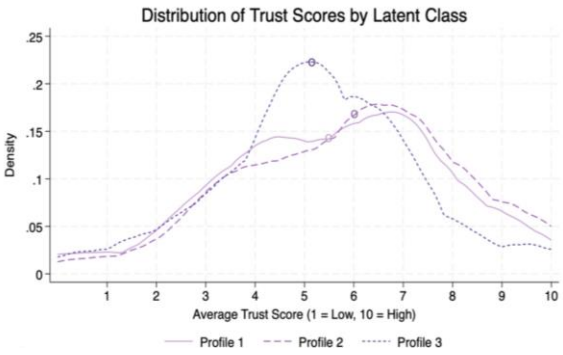

Conclusions. This study demonstrates how trust in public health authorities varies across the U.S. population in patterned and intersectional ways. LCA and regression models show that trust is not uniformly distributed, even among groups with similar resources, and is shaped by structural factors such as race, education, insurance status, and geography. Together, these results support an intersectionally-informed view: structural domains explain average differences, but effects are profile specific. Therefore, one-size-fits-all strategies to address (mis)trust risk overlooking inequities. Future research should incorporate qualitative methods and consider longitudinal data to better understand how trust develops, shifts over time, and responds to social and institutional change.

Enhancing critical infrastructure networks resilience against extreme weather events using multicriteria portfolio decision analysis

Joaquín de la Barra, Aalto University, Finland
Email: joaquin.delabarra@aalto.fi
IIASA Mentors: Piotr Zebrowski (ASA) and Stefan Hochainer-Stigler (ASA)

Introduction. Advanced societies rely heavily on critical infrastructure networks (CINs) to provide essential goods and services. Extreme weather events jeopardize the integrity of CINs, resulting in temporary or prolonged service disruptions. The reliability of a CIN is its ability to maintain services during such disruptive events, while resilience is its ability to restore the services after disruptions. When services are interrupted, the CIN performance degrades until the services are restored. The cumulative performance loss (until time of restoration) is a widely used metric of CIN's resilience [1]. In this project, we propose a multicriteria decision analysis framework designed to support the cost-efficient allocation of resources toward portfolios of fortification actions that simultaneously maximize reliability and minimize expected performance loss.

Methodology. Using minimal path sets and minimal cut sets, we developed an algorithm to identify sequences of restoration actions on disrupted nodes of a CIN that minimize performance loss. This allowed us to derive a surrogate function that approximates the expected cumulative performance loss of the CIN as a function of the failure probability of its components. Since the CIN's reliability is also a function of these probabilities, we framed the selection of fortification portfolios as a problem of simultaneous maximization of reliability and minimization of expected cumulative performance loss. Using a surrogate function for expected cumulative performance loss, we identify candidate Pareto-optimal portfolios of fortification actions. Next, using Monte Carlo simulations to generate multiple failure scenarios for all candidate portfolios, we obtain a more accurate estimate of expected cumulative performance loss and discard Pareto-dominated (suboptimal) ones.

Results. We study the fortification of the Siilinjärvi railway station in Finland against extreme weather events, using illustrative values for failure probabilities and costs. The station provides three services, each defined as a connection between its terminal points. The overall reliability and expected performance loss for the station are computed as weighted sums of each connection's reliability and expected cumulative performance loss, where the weights reflect the relative importance of each connection. Candidate fortification portfolios, identified by co-optimizing reliability and a surrogate cumulative performance loss function, are shown in the left panel for various budget levels. The Pareto-optimal portfolios, identified by filtering the candidates based on expected cumulative performance loss, are presented in the right panel.

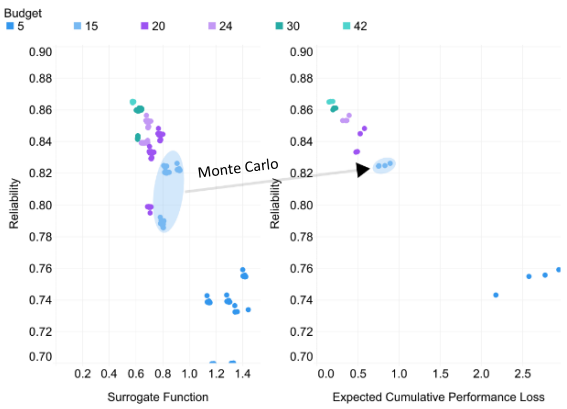

Conclusions. The proposed framework is generic and can be employed to identify fortification portfolios that enhance the reliability and resilience of CINs (not only railway networks). Results demonstrate the added value of investigating trade-offs and synergies between the reliability and resilience of the CINs. Our case study suggests that for small budgets, a slight compromise on reliability can result in a significant improvement in resilience.

References

[1] Cui, X., Li, B., Zhang, S., Ji, Z., Wang, S., Luo, R., Ren, Y., & Xiao, Y. (2025). Resilience-Based Restoration Sequence Optimization of Disrupted Transportation Networks: A Novel Mathematical Approach. Transportation Research Part D: Transport and Environment, 145, 104834. https://doi.org/10.1016/j.trd.2025.104834

A novel single and double-cropping rice mapping method by integrating phenology knowledge and deep learning without current-year ground samples

Xinyu Zhang, Huazhong Agricultural University, China
Email: zxy0119@webmail.hzau.edu.cn
IIASA Mentor: Juan Carlos Laso Bayas (ASA)

Introduction. Rice contributes around 8% of human-related methane and sustains over 3.5 billion people globally. In China, the disappearance of triple-cropping rice and the large-scale shift from double-cropping (DC-Rice) to single-cropping rice (SC-Rice) have reduced cropland use efficiency, threatening food security. Timely and accurate mapping of SC/DC-Rice is critical for crop structure adjustment, yield estimation, water management, and greenhouse gas assessment, yet is hindered by limited current-year samples. We propose PhenoDeep, which integrates phenology-based decision rules, K-means clustering, and unique spectral histogram relationships to generate fine samples via a U-net model, enabling accurate multi-year SC/DC-Rice mapping with Random Forest.

Methodology. PhenoDeep generates potential SC-Rice and DC-Rice samples using prior agricultural phenology knowledge, then identifies their topological relationships in spectral histogram space, guided by the Separability Index. These sample sets are standardized to ensure consistent relationships across years, and high-quality target-year samples are produced via a U-Net semantic segmentation model. The Random Forest algorithm maps rice cropping patterns using these samples.

Results. Using prior phenological knowledge and deep learning, PhenoDeep achieved high-precision mapping of SC-Rice and DC-Rice. Pre-classification based on growth peak frequency and flooding indicators reduced manual interpretation, while spectral-temporal separability analysis optimized feature selection and captured topological relationships in feature space. Generated samples reduced the average standard deviation of LSWI and NDVI time series by 6.3%-10.1%, improving classification reliability. Trained on 2018-2020 samples and applied to 2015 and 2021 in Dongting lake plain, PhenoDeep achieved overall accuracies of 92.41% and 90.35% with F1-scores of 0.93 and 0.88, demonstrating strong temporal transferability.

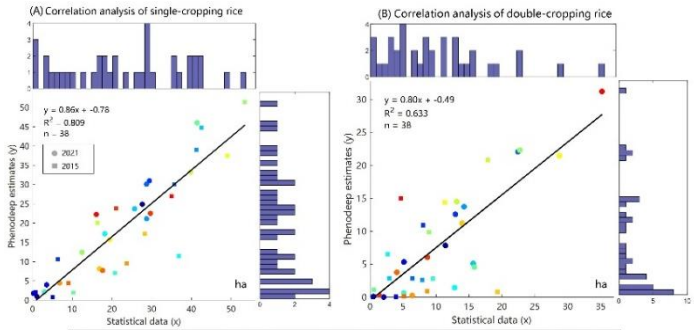

Fig.1 Correlation between statistical rice area data and PhenoDeep estimates for county-level statistical data in the Dongting Lake Plain (2015 and 2021) PhenoDeep-RF maps in Dongting Lake Plain.

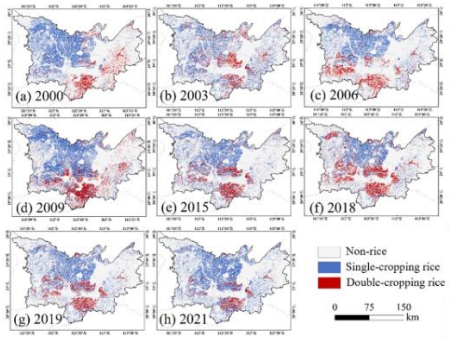

Fig.2 Historical PhenoDeep-RF maps in Dongting Lake Plain.

Conclusions. Through spatiotemporal mapping, this study found that 5,785.6 km² DC-Rice transition to SC-Rice in southern China between 2009 and 2016. This transition was accompanied by a reduction of 174,000 in labour input and a decrease of 1,146 kt in carbon emissions, but also resulted in a loss of 6.7 billion CNY in income and a yield reduction of 2,488 kt, creating a substantial calorie gap equivalent to the annual food demand of 27 million people. Addressing the implications of such transitions requires policies that carefully balance productivity, food security, and the urgent need for climate change mitigation.

How intensively are Europe's forests managed? towards a database and framework for tracking indicators, addressing uncertainty, and capturing change

Florian Weidinger, BOKU University, Austria
Email: florian.weidinger@boku.ac.at
IIASA Mentors: Linda See (NODES) and Fulvio Di Fulvio (BNR)

Introduction. Forests play a crucial role in global carbon cycles, acting as sinks or sources depending on management and natural dynamics. Europe's forests store a large share of the continent's biomass carbon but face growing anthropogenic and environmental pressures. Analysing the interactions between forest management and carbon dynamics requires reliable ground-based data, yet inconsistencies between national reporting and forest inventories hinder pan-European comparisons. Although harmonisation efforts exist, there is currently no consistent time series dataset from ground-based sources that captures key forest metrics for forest biomass dynamics at an adequate temporal and spatial scale. This research addresses the challenges and uncertainties in creating such a harmonised dataset from a previously compiled database of reported National Forest Inventory (NFI) and census data (EUFo-reported) on forest area, growing stock, increment and harvest, from 2000-2022, covering 93% of EU27 forest area at subnational level.

Methodology. Constructing the "EUFo-harmonised" dataset from EUFo-reported requires solving two main problems: (i) conversion to uniform units and (ii) gap filling for non-reported years. For (i), expansion and conversion factors were compiled to estimate, e.g., bark and harvest residues, and to convert volumes to masses. For (ii), time-series data from FAO and SoEF ("State of European Forests") supported gap filling for area and harvest, while biomass stock and increment gaps were modelled with the bookkeeping model *CRAFT*. Although harmonisation is ongoing, the database already allows calculations of forest management intensity as averages over periods. To test potential applications, intensity indicators were correlated to a remotely-sensed map of forest management categories (Scherpenhuijzen et al., 2025).

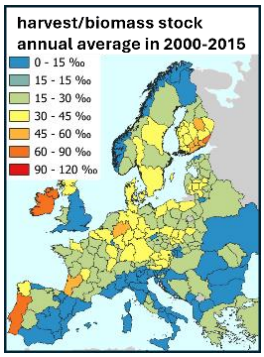

Results. Harmonisation and gap filling for forest area and harvest produced satisfactory results, matching FAO and SoEF totals at the European level, although notable country-level differences remain (e.g., DE, IT). Biomass harmonisation proved more challenging. Existing harmonised datasets were of limited use due to spatial and temporal mismatches to EUFO-reported. *CRAFT* provided robust interpolations but overestimated the extrapolated values. Reported increment data were sparse and often unclear (gross vs. net), hence, harmonised increment was calculated as the sum of stock difference and harvest. While EUFo-reported growing stock volumes align with FAO and SoEF, aboveground biomass carbon estimates had large discrepancies between sources and between different expansion and conversion factors, ranging in EU27(excl. Malta) from 12GtC to 18BtC (averaged 2000-2020). Among calculated intensity indicators (harvest/area, harvest/increment, harvest/stock) for the averaged period 2000-2015, harvest/stock showed correlations with the forest management categories.

Conclusion. Creating a consistent, harmonised time series for key forest indicators in Europe is challenging, as NFIs and censuses lack standardised reporting. There are no "one size fits all" solutions, which also makes the work technically complex. Although biomass stock harmonisation is ongoing, current uncertainties already underscore the need for caution in forest harvest practices to maintain Europe's forests as a carbon sink - especially given the rising demand to substitute fossil fuels and substitution of concrete with wood as a building material. However, comparing forest management intensities with remotely sensed products has already provided valuable insights to guide future research and improve our understanding of Europe's forests.

References

CRAFT: Le Noë, J., Matej, S., Magerl, A., Bhan, M., Erb, K. H., & Gingrich, S. (2020). *Global Change Biology*, *26*(4), 2421–2434. Scherpenhuijzen, N., West, T. A. P., Debonne, N., Oostdijk, S., Adame, P., Astrup, R., & Verburg, P. H. (2025). *Forest Ecology and Management*, *594*, 122940.

Analyzing requirements for an accurate land cover data collection by visual interpretation of various sources of images

Ana Paula Matos e Silva, Federal University of Goiás, Brazil
Email: anapaulam@ufg.br
IIASA Mentors: Myroslava Lesiv (ASA) and Steffen Fritz (ASA)

Introduction. Land use and land cover (LULC) mapping plays a crucial role in understanding environmental dynamics, informing public policy, and supporting territorial management. Visual interpretation of satellite imagery, although often indispensable, faces significant challenges. Differences among sensors—in spatial, spectral, and temporal resolution—affect the ability to distinguish features and classes, while class assignment itself involves subjectivity, as interpreters may apply different criteria. These factors compromise product consistency and comparability. In this context, the present study examines how different imagery sources and ancillary information influence the quality of visual interpretation and the reliability of resulting maps.

Methodology. We run a few experiments comparing results of visual interpretation of various sources of images for four scenarios: (1) Landsat (30 m), (2) Sentinel-2 (10 m), (3) Google VHR, and (4) Google VHR with supplementary information. The study covered 3 regions, Europe, Africa, and Brazil, representing large and diverse global regions. For each study region, a total of 2,000 points were uniformly distributed among the eight ESA WorldCover classes: Tree cover, Cropland, Built-up, Wetland, Shrub cover, Grassland, Bare land/sparse vegetation, and Water. Visual interpretation was carried out using two established tools: Geo-Wiki, which provides access to high-resolution imagery, and TVI (Temporal Visual Inspection), designed for temporal analysis of lower-resolution imagery. The interpretation team comprised five experts with varying levels of experience, including three from the IIASA and two from the Remote Sensing and GIS Lab (LAPIG). Sample points were randomly distributed among the experts, and each sample point was interpreted once.

Results. Overall, 41% of sample points matched across all imagery scenarios, while 10% differed only in Landsat, 8% only in Sentinel-2, and 7% where Landsat and Sentinel-2 agreed but high-resolution imagery indicated a different class. Just 2% showed completely different classes in all cases. We observed the highest agreement between the annotations in Brazil , followed by Europe and Africa. The analysis of disagreement causes indicates multiple contributing factors, including interpreter's mistakes, limitations associated with coarse spatial resolution, insufficient information due to unfavorable image acquisition dates(Fig.1), the presence of clouds or atmospheric interferences, class changes throughout the year, and, in some cases, the heterogeneity of land cover within a single 30 × 30 meter cell, containing multiple elements such as trees, shrubs, built-up areas, bare soil, and grasslands.

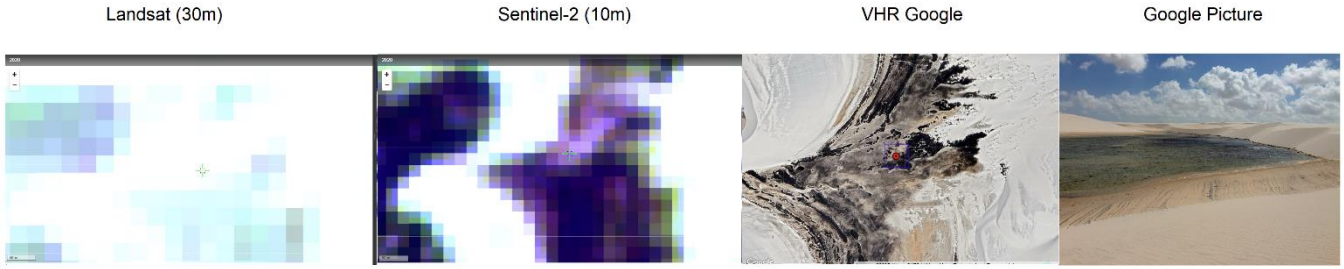

Figure 1. Example of a landscape whose visual classification varies according to image resolution and acquisition date.

Conclusions. The experiment demonstrated that, although there is a considerable level of agreement across different imagery sources and resolutions, discrepancies persist due to technical limitations, acquisition conditions, and the complexity of landscapes, including anthropogenic changes within the year. The findings highlight the importance of selecting appropriate imagery types and complementary information for each mapping context, to optimize the accuracy and consistency of LULC products.

Revealing the indirect impacts of climate change on high-latitude countries: An integrated climate and economic model approach

Zhenjun Zhang, Beijing Institute of Technology, China
Email: zhangzhenjun0118@163.com (home email)
IIASA Mentors: Khabarov Nikolay (ASA) and Stefan Hochrainer-Stigler (ASA)

Introduction. Global climate change is a common challenge faced by all of humanity. In recent years, the international community has taken a series of measures to address it. For example, the Paris Agreement set a goal of limiting global warming to 1.5°C, and more than 150 countries have proposed carbon neutrality goals. However, the impacts of climate change vary across countries. For instance, high-latitude countries may experience some positive effects in the short term, which could weaken their enthusiasm for emission reduction. However, the production processes of goods worldwide are highly complex. The direct impacts of temperature rise on individual countries may be transmitted to others through global supply chains. The indirect economic impacts behind the direct effects of temperature rise on agricultural production urgently need to be uncovered in order to prompt global emission reduction actions.

Methodology. First, we obtain the future results (2030–2099) of the EPIC-IIASA model under three scenarios (SSP126, SSP370, SSP585) for four types of crops (maize, rice, soybean, wheat). These results are then organized into country-level data and matched with the regions and sectors in the GTAP global multi-regional input–output table, with physical quantities converted into value terms. Next, the total output data from the EPIC-IIASA results are allocated between intermediate demand and final demand, with the final demand portion further distributed across national consumption. Finally, by applying the multi-regional input–output model, we estimate the GDP generated through global supply chains by countries' final consumption of crops.

Results. Compared with the SSP126 scenario, under the SSP370 scenario most countries will suffer direct losses from temperature rise, while Argentina, Australia, Eastern European countries, and Southern Africa may benefit to some extent. However, global supply chains transfer most of these benefits to high-income regions such as the United States, Canada, the European Union, and Japan. Under the SSP585 scenario, global losses increase further, with the EU gaining additional benefits through global supply chains, while developing countries such as China, India, and Pakistan experience significant losses, thereby further exacerbating global inequality. Under global warming scenarios, high-latitude countries may initially benefit from increased crop yields, but as global temperatures continue to rise, these countries will eventually suffer adverse effects.

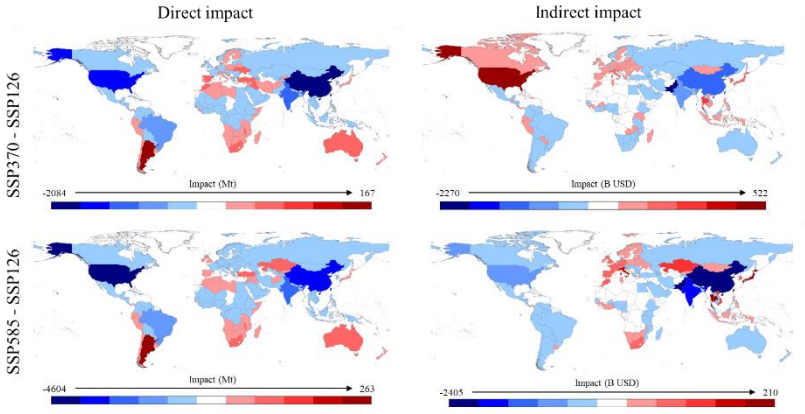

Conclusions. Under global warming scenarios, agricultural output and its economic impacts exhibit clear imbalances. High-latitude countries may initially benefit from yield increases, but prolonged warming will eventually bring adverse effects. In contrast, most low- and mid-latitude countries face yield losses, with direct damages transmitted through global supply chains, worsening the situation for developing economies. Moreover, supply chains shift part of the benefits toward high-income regions, further intensifying global inequality. These findings highlight that climate change is not only an environmental issue but also a major challenge for global economic equity, underscoring the urgency of coordinated mitigation and adaptation efforts.

Forest age dynamics in OSCAR: Improving land use emission estimates and reconciliation with national inventories

Yuqin Lai, Peking University, China
Email: laiyq@pku.edu.cn
IIASA Mentor: Thomas Gasser (ASA, ECE) and Biqing Zhu (ASA, ECE)

Introduction. Emissions from land-use change (ELUC) are critical to the global carbon cycle. Bookkeeping models (BMs) are essential tools in the Global Carbon Budget (GCB) for estimating these emissions. However, traditional BMs ignore that forest carbon sequestration is **age-dependent**, limiting their accuracy. This methodological gap contributes to persistent model-inventory gap, complicating reconciliation efforts.

Methodology. We developed and implemented a novel forest age dynamics module within OSCAR, one of three BMs used in the GCB. The module explicitly tracks forest area across multiple age classes, simulating five key drivers of age structure: natural aging and mortality, land-use change, harvesting, and shifting cultivation. To capture ecological reality, age class boundaries are defined by a biomass-based strategy, ensuring higher resolution during the rapid growth phases of young forests. This age structure then modulates the carbon cycle via an age-weighted adjustment to Net Primary Productivity (NPP), linking a forest's growth stage to its carbon uptake capacity. The model was initialized to a pre-industrial steady state (1750) and run with historical forcings to 2014, followed by future projections to 2100 under various scenarios.

Results. Historical simulations reveal that incorporating forest age dynamics systematically lowers estimated land-use emissions by revealing a stronger carbon sink than previously modeled. For the critical 2005-2014 period, the age-aware model reduced the estimated net carbon source by **0.2585 PgC/yr**, a **22.8% decrease** compared to the baseline model. This emission difference is highly significant, as it accounts for **17.2% of the total gap** between bookkeeping models and national inventories, and resolves approximately **57% of the previously unexplained residual portion** of this gap. Future projections under various SSP scenarios consistently show that the enhanced carbon sink from the current global forest age structure is a transient phenomenon that will **diminish as forests mature**. This highlights the temporary nature of this ecosystem service.

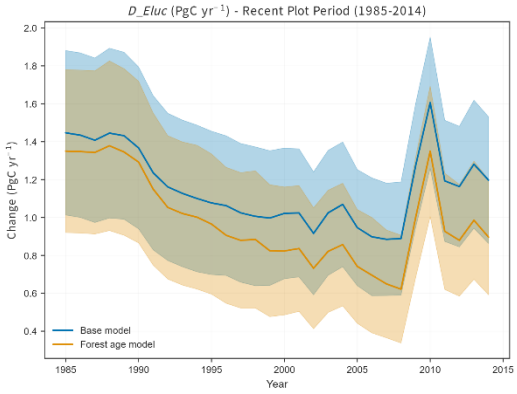

Comparison of land-use emissions (ELUC) for the recent historical period (1985-2014).

Conclusions. We enhanced an advanced bookkeeping model by incorporating a comprehensive forest age dynamics module. Our historical reconstructions yielded refined land-use change emission (ELUC) estimates and quantified age-related impacts on the carbon cycle. Through systematic comparison with NGHGIs, we demonstrated that explicitly accounting for age structure is crucial for resolving persistent model-inventory discrepancies. By pioneering this integration, our findings not only improve carbon quantification precision but also provide critical insights to inform future climate policy, support the Global Stocktake, and guide land-based mitigation investments.

References

Gidden, M. J., Gasser, T., Grassi, G., Forsell, N., Janssens, I., Lamb, W. F., Minx, J., Nicholls, Z., Steinhauser, J., & Riahi, K. (2023). Aligning climate scenarios to emissions inventories shifts global benchmarks. Nature, 624(7990), 102–108. https://doi.org/10.1038/s41586-023-06724-y

Grassi, G., Stehfest, E., Rogelj, J., van Vuuren, D., Cescatti, A., House, J., Nabuurs, G.-J., Rossi, S., Alkama, R., Viñas, R. A., Calvin, K., Ceccherini, G., Federici, S., Fujimori, S., Gusti, M., Hasegawa, T., Havlik, P., Humpenöder, F., Korosuo, A., … Popp, A. (2021). Critical adjustment of land mitigation pathways for assessing countries' climate progress. Nature Climate Change, 11(5), Article 5. https://doi.org/10.1038/s41558-021-01033-6

Modelling semi-arid ecosystem processes in Baringo County, Kenya using the BGC-MAN model

Protus Kyalo, Lukenya University, Kenya
Email: pmutuku100@gmail.com
IIASA Mentors: Stephan Pietsch (ASA) and Zebrowski Piotr (ASA)

Introduction. Semi-arid lands in Kenya face increasing stress from deforestation, land degradation and extreme weather. In Baringo County, Landsat-based analyses show large expansion of cropland and shrub (+1196km^2 cropland) alongside declines in forest and grassland cover[1]. These changes are driven by deforestation, invasive *Prosopis* spread and population-driven fuel demand which have degraded soil quality and carbon stocks[2]. The BGC-MAN model, which integrates soil-plant biogeochemistry and management actions, has emerged as a critical tool for understanding tree growth under varying conditions. We apply BGC-MAN to simulate tree and soil carbon in Baringo's ASALs, informing restoration and land use decisions.

Methodology. We prepared site-specific inputs for 43 sample sites in Baringo County. Tree cover percentage was obtained from MODIS Vegetation Continuous Fields (VCF) at 250m resolution. Laboratory-tested field soil data was complemented by data from the harmonized world soil database[4]. Using literature values for population increase and fuel use[2], we estimated historical fuel wood extraction (thinning) rates. A Monte Carlo approach sampled population-driven thinning scenarios to provide realistic representation of human impact on carbon dynamics. The BGC-MAN model was run for each site with local climate and soil inputs to simulate daily carbon, water and nitrogen fluxes. Outputs (annual tree biomass carbon and soil organic carbon) were aggregated and compared to observed values for validation.

Results. No significant difference between observed and predicted output values for tree carbon (t(43)=0.046, p=0.963>0.05, Cohen's d = 0.007<0.01) and soil carbon (t(43)=0.051, p=0.960>0.05, Cohen's d= =0.008<0.01) were found. Figure 1and 2 depict graphs by year at selected sites which demonstrates the model's ability to capture land-degradation effects, including declines linked to drought years (1975, 1984, 1991, 2004)[3]. The simulations also reveal heterogeneity across sites, reflecting differences in fuelwood extraction pressure and recovery dynamics.

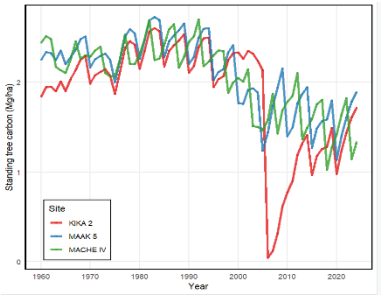

Figure 1: Standing Tree carbon by time

Conclusions. The BGC-MAN reliably reproduces observed carbon dynamics in Baringo's semi-arid ecosystems, for both tree and soil carbon outputs. The model exhibits sensitivity to both human land use and climate change impacts by reproducing stable, declining and partially recovering trajectories as they were observed in Baringo county during past droughts[3]. Future work will include shrubs and grasses and use more validation metrics to make regional applications more robust.

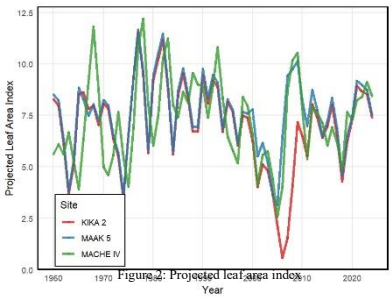

Figure 2: Projected leaf area index

References

[1] Kipkulei H, Rotich B, Ahmed A, Lameck AS, Burudi J, et al. (2025). Land use/land cover dynamics in an arid and semi-arid landscape: a 24-year analysis of Baringo County, Kenya (2000–2024). *Global and Earth Surface Processes Change*, 4:100006.
[2] Otieno R, Bager L, Odhiambo V, Wanjohi B (2022). Adoption of Improved Biomass Cook Stoves: Case Study of Baringo and West Pokot Counties in Kenya. *Journal of Sustainable Bioenergy Systems*, 12(2)
[3] Ochieng, R., Recha, C., & Bebe, B. O. (2017). Rainfall variability and droughts in the drylands of Baringo County, Kenya. Open Access Library Journal, 4, 1-15. doi: 10.4236/oalib.1103827.
[4] FAO/IIASA/ISRIC/ISSCAS/JRC, 2012. Harmonized World Soil Database (version 1.2). FAO, Rome, Italy and IIASA, Laxenburg, Austria

Mexico's agricultural socio-ecological and socioeconomic footprint archetypes.

Daniel Itzamna Avila-Ortega, Stockholm Resilience Centre, Stockholm University, Sweden
Email: daniel.avila@su.se
IIASA Mentors: Valeria Javalera Rincón (ASA) and Sören Lindner (ASA)

Introduction. Conventional agriculture, with its heavy reliance on agrochemicals, technology and extensive practices, poses significant threats to biodiversity, human health, and largely contributes to climate change, biodiversity loss and land use change[1–7]. Yet, its role in providing widespread and affordable food is undeniable[8], creating a critical dichotomy with alternative, agroecological systems. The transition to sustainable farming is fraught with challenges, including high labour demands and (bio)inputs, and structural barriers, highlighting the urgent need for new approaches. Particularly, since both systems underpin differentiated socio-economic and socio-ecological profiles in their production practices. This study explores this complex issue by analysing the socioeconomic and socio-ecological footprints of differentiated farming practices in Mexico.

Methodology. To explore the diversity of agricultural practices and their corresponding profiles, we processed a dataset of over 60,000 farms in Mexico. We first assembled a relational SQLite database that included socio-economic and environmental variables. To identify commonalities in agricultural practices, we performed a combined Factor Analysis for Mixed Data (FAMD) and a Clustering for LARge Applications (CLARA) analysis on the raw data. This allowed us to group farms with similar characteristics into archetypes.

Results. Our analysis identifies 63,000 plot-year records in Mexico spanning over 10 years (2012-22). Most plots are rainfed (~76%), 98% are single-crops (with 80% cultivating maize), and 90% belong to the summer cycle (April - September). Farmers are 84% male and 16% female; 49% have elementary education, and 13% no formal education. Land tenure is 67% within ejidos, 23% private property, and the rest is community. In total, 83% is legally owned, whereas 12% rent the land and 4% borrow it. We identified seven farming archetypes clearly distinguished by the water regime, either rainfed (1,2,5) or irrigation (3,4,6,7): (1) Low-input baseline, (2) Application-intensive, (5) Operation/fertiliser-heavy; (3) Irrigation-dominant/mechanised, (4) Balanced intensification, (6) Water-driven/low-chemical, and (7) Maximal intensification (water+machines+inputs).

Conclusions.
No single production model defines the Mexican agricultural landscape. Our analysis reveals seven distinct archetypes, spanning from low-input rainfed (Arch 1) to maximal-intensification (Arch 7). This spectrum highlights a key trade-off, with farms intensifying via operations (rainfed) or capital (irrigated). These distinct socio-ecological "footprints" prove that policies must be designed according to the required production models and outputs, as there is no such thing as a one-size-fits-all "conventional" or "agroecological" farm.

References

Clark, M. A., & Tilman, D. (2017). *Environmental Research Letters*, *12*.
IPBES. (2019). *Summary for policymakers of the global assessment report on biodiversity and ecosystem services* (No. IPBES 7; IPBES Plenary at Its Seventh Session). Intergovernmental Science-Policy Platform On Biodiversity And Ecosystem Services.
IPCC. (2019). Summary for Policymakers. Shukla, et al., (Eds.), *Climate Change and Land: An IPCC special report on climate change, desertification, land degradation, sustainable land management, food security, and greenhouse gas fluxes in terrestrial ecosystems.* Cambridge University Press.
Usubiaga-Liaño, A., Mace, G. M., & Ekins, P. (2019). Limits to agricultural land for retaining acceptable levels of local biodiversity. *Nature Sustainability*, *2*(6), 491–498.
Ortiz, A. M. D., Outhwaite, C. L., Dalin, C., & Newbold, T. (2021). A review of the interactions between biodiversity, agriculture, climate change, and international trade: Research and policy priorities. *One Earth*, *4*(1), 88–101.
Devi, P. I., Manjula, M., & Bhavani, R. V. (2022). *Annual Review of Environment and Resources*, *47*(1), 399–421.
Rasul, K., Bruckner, M., Mempel, F., Trsek, S., & Hertwich, E. G. (2024).. *PNAS Nexus*, *3*(12), pgae524.
Duinen, G. V. (2008). *Nature Geoscience*, *1*.

Demand-side flexibility for balancing microgrids in islanded mode: engaging local consumers in resilient energy transitions

Anzhelika Slobodian, Institute of Electrodynamics of the National Academy of Sciences of Ukraine
Email: anslobodyan@gmail.com
IIASA Mentors: Tatiana Ermolieva (ASA) and Nadejda Komendantova (ASA)

Introduction. Frequent large-scale outages in Ukraine and across Europe highlight the vulnerability of centralized power systems. In Ukraine, targeted attacks on energy infrastructure underscore the need for resilient, locally autonomous solutions. Demand-side flexibility (DSF) — the ability of consumers to adjust electricity use in response to system needs — can help microgrids in islanded mode both maintain essential services and increase electricity availability for households. In this study, potential DSF was modelled relative to simulated PV generation, enabling optimisation of consumption according to available supply. 90 scenarios were analysed for a small municipality in western Ukraine, assessing how different DSF levels improve microgrid balance under varying seasonal and weather conditions.

Methodology. A microgrid model was developed in MATLAB, with predominantly residential demand and local solar PV generation simulated in SAM. 90 scenarios were analysed, representing peak consumption days in winter and summer under cloudy, sunny, and average weather conditions. Three consumer behaviour strategies were assessed: baseline (no flexibility), a 3.4% demand shift based on Norwegian price-response studies[1], and a maximum feasible flexibility scenario considering technical limits of residential users and critical infrastructure. Each case was simulated for both continuous outages and scheduled disconnections to evaluate impacts on energy balance and load supply.

Results. In July, with existing storage capacity, the microgrid could fully supply critical infrastructure in all scenarios. Under the 3.4% DSF case, only 1% of residential load was additionally served, while the maximum feasible DSF enabled 3–11% more electricity delivery to households. In January, cloudy days prevented full supply to critical infrastructure, even with maximum DSF, due to insufficient PV generation for battery charging. However, on sunny winter days, DSF increased residential coverage by 1–8% (Norwegian level) and 1–18% (maximum feasible level). For average and cloudy winter days under scheduled outages, gains were limited to 1–2% and 10–16% respectively.

Conclusions. This study shows that DSF is a significant factor in improving the operational resilience of islanded microgrids. Even modest flexibility levels yield measurable improvements in load coverage, while higher responsiveness substantially increases electricity supplied to both critical infrastructure and households. The modelling results indicate that in high-response scenarios, battery cycling and usage duration are reduced, and the battery retains sufficient charge at the end of the day to continue supplying the microgrid, in contrast to the baseline case. DSF also enables more efficient use of available generation by reducing PV curtailment, which is particularly valuable for systems with high renewable penetration. This can lower the need for additional storage capacity and help stabilise electricity costs for end-users, while strengthening community-level energy security.

References

[1]Hofmann, M., & Lindberg, K. B. (2024). Evidence of households' demand flexibility in response to variable hourly electricity prices – Results from a comprehensive field experiment in Norway. Energy Policy, 184, 113821.

Social-ecological network analysis of meadow governance in Sweden

John Lind, Mid Sweden University, Sweden
Email: john.lind@miun.se
IIASA Mentors: Nikita Strelkovskii (ASA) and Brian Fath (ASA)

Introduction. Meadows are among the most highly biodiverse ecosystems; once a crucial agricultural production form, meadow land has been heavily reduced in Sweden over the last century. While land definitions have shifted over time, one estimate shows a ~97% reduction between 1927-2020 (Jordbruksverket 2023). A reduction of meadows suggests a reduction of the combined ecosystem services they provide, such as food production, recreation, and regulation of the environment. This study aims to investigate public sector meadow governance in Sweden using social-ecological network analysis (SENA) with an ecosystem services (ES) perspective.

Methodology. We utilize the Common International Classification of Ecosystem Services (CICES) to list which ES are present on meadows. A spatially neutral, minimalist conceptual approach was developed: ES were included based on the possibility to be present on any meadow based on a typical definition, rather than empirical examples. ES were defined as nodes and unweighted edges were established based on one-step distance in trophic connection per energy systems language category (Odum 1983). Governance actors were web-scraped from the government offices website *regeringen.se*, and connected based on co-occurrence per post featuring search words containing "meadow" and "mowing" in Swedish. Edges between governance actors and ecosystem services were defined based on stated objectives in the posts paired with equivalent ES. SENA was then performed in RStudio.

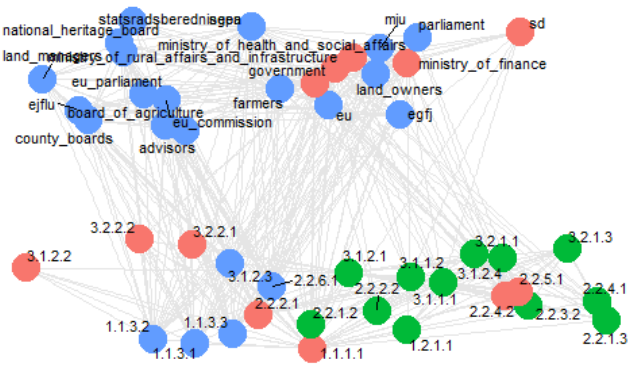

Results. The ES nodes with the highest degree, betweenness and eigenvector are cultivated terrestrial plants grown for nutritional purposes (CICES code 1.1.1.1) present on meadows in the form of vegetation and later hay, and 3.1.2.1: Characteristics of living systems that enable scientific investigation or the creation of traditional ecological knowledge, as this span system-wide. The government offices have the highest degree, betweenness and eigenvector, followed by the Environmental Protection Agency, Ministry of Climate and Enterprise, and Board of Agriculture. Community detection revealed three communities (see fig. 1), relatively ungoverned ES, a national set of actors governing ES connected to objectives of biodiversity, and a third cluster of more peripheral governance actors together ES in climate change and the biomass category. The network has a matching degree of 0.375 on a scale from 0 to 1. A higher matching degree is considered to reduce adverse impacts on natural resource systems (see Zhang et al 2019).

Conclusions. The central role of the government offices node was expected since it is the data source - subsequently listed social nodes reveal central actors targetable for improving future meadow governance. Isolated ES nodes are possibly neglected and may benefit from targeted governance. The social layer clusters could collaborate to increase holism of meadow governance. Future analysis will show the most effective collaborations among governance actors to increase the matching degree.

References

CICES. (n.d.). CICES – Towards a common classification of ecosystem services. https://cices.eu/
Jordbruksverket (2023). Ett rikt odlingslandskap – fördjupad utvärdering 2023. Rapport 2022:17 from https://www2.jordbruksverket.se/download/18.7045f0cf184c20a13ed500a8/1669795787915/ra22_17.pdf
Odum, H.T. (1983). Systems ecology: An introduction. New York: Wiley.
Zhang, M., Wang, S., Fu, B., Wei, X., Wang, C., Song, S., & Wei, F. (2019). Sustainability, 11(19), 5159.

Index